

**NON-DESTRUCTIVE MANGOSTEEN GRADING USING  
IMAGE PROCESSING AND NEAR-INFRARED  
SPECTROSCOPY (NIRS)**

**ANJALI ACHARYA**

**A THESIS REPORT SUBMITTED IN PARTIAL FULFILLMENT  
OF THE REQUIREMENTS FOR THE DEGREE OF  
MASTER OF ENGINEERING IN COMPUTATIONAL INTELLIGENT SYSTEMS  
INTERNATIONAL COLLEGE  
KING MONGKUT'S INSTITUTE OF TECHNOLOGY LADKRABANG  
ACADEMIC YEAR 2018  
KMITL-2018-IC-M-11-08**

**NON-DESTRUCTIVE MANGOSTEEN GRADING USING  
IMAGE PROCESSING AND NEAR-INFRARED  
SPECTROSCOPY (NIRS)**

**ANJALI ACHARYA**

**A THESIS REPORT SUBMITTED IN PARTIAL FULFILLMENT  
OF THE REQUIREMENTS FOR THE DEGREE OF  
MASTER OF ENGINEERING IN COMPUTATIONAL INTELLIGENT SYSTEMS  
INTERNATIONAL COLLEGE  
KING MONGKUT'S INSTITUTE OF TECHNOLOGY LADKRABANG  
ACADEMIC YEAR 2018  
KMITL-2018-IC-M-11-08**

COPYRIGHT 2018

INTERNATIONAL COLLEGE

KING MONGKUT'S INSTITUTE OF TECHNOLOGY LADKRABANG

# Abstract

Mangosteen is one of the fruits that has an enormous export potential in Thailand. It is known as the queen of fruit. Mangosteen export generates large revenue; however, fruit is not defect free it contains many undesirable external as well as internal condition which results in the shipment rejection and decrease the reliability of the export. This research investigates a novel classification approach for surface defect detection and nondestructive prediction of internal defects such as translucent disorder (TD) and presence of yellow gummy latex (YG) of mangosteen.

In this research, for the first time, we mainly focus on the external and internal defects. The application of texture features extracted from gray level co-occurrence matrix and deep learning self learned features for the external defect classification based on Image processing and Near-Infrared Spectroscopy (or called NIRS) for internal defects classification respectively. There are 3 classes of surface roughness namely Glossy Surface (GS), Medium Rough surface (MR) and Extreme Rough surface (ER). For the determination of internal defects we consider 2 major defects prevailing in the export industry which are translucent disorder (TD) and yellow gummy latex (YG). TD is mainly caused by excessive water content in fruit pulp and latter is identified by the presence of yellow gum like substance either in pericarp, fruit pulp or both.

# Acknowledgments

Firstly, I would like to express my sincere gratitude to Dr. Montri Phothisonothai, my project advisor, for the continuous support of my masters study research, for his patience, motivation, and immense knowledge. His guidance helped me all the time of my research and writing of this thesis. I could not have imagined having a better advisor and mentor for my research. I would also like to thank Dr. Suchada Tantisatirapong, for her advice in using different techniques and technologies in this study and accompanying us during data collection.

I would also like to thank Asst.Prof.Dr. Chaiwat Nuthong, Dr. Ukrit Watchareeruetai for their constant feedback in seminar session and all lecturers of International College, KMITL who have provided the proper knowledge to complete my coursework and research studies.

Finally, I must express my very profound gratitude to my parents and to my friends for providing me with unfailing support and continuous encouragement throughout my years of study and through the process of researching and writing this thesis. This accomplishment would not have been possible without them. Thank you.

# Table of Contents

<b>1</b>	<b>Introduction</b>	<b>1</b>
1.1	Background . . . . .	1
1.2	Problem Descriptions . . . . .	1
1.3	Research Objectives . . . . .	2
1.4	Scope . . . . .	3
<b>2</b>	<b>Literature Review</b>	<b>5</b>
2.1	Computer vision and Image processing . . . . .	5
2.2	Texture Analysis . . . . .	5
2.3	Surface defect detection of fruits . . . . .	6
2.4	Internal defects of Mangosteen . . . . .	10
2.4.1	Near Infrared Spectroscopy . . . . .	10
<b>3</b>	<b>Background Knowledge</b>	<b>13</b>
3.1	Mangosteen . . . . .	13
3.2	Gray Level Co-occurrence Matrix . . . . .	13
3.3	Deep Learning . . . . .	15
3.3.1	Convolution Neural Network . . . . .	15
3.3.2	Transfer Learning . . . . .	15
3.4	Near Infrared Spectroscopy . . . . .	16
3.4.1	Working Principle . . . . .	16
3.4.2	NIR Sensors . . . . .	17
3.4.3	AS7263 NIR Sensor . . . . .	17

<b>4</b>	<b>Methodology</b>	<b>19</b>
4.1	Data Collection . . . . .	19
4.2	External defect:surface roughness . . . . .	19
4.2.1	Image Acquisition and Pre-processing . . . . .	21
4.2.2	Region Of Interest . . . . .	21
4.3	Gray Level Co-occurrence Matrix . . . . .	21
4.3.1	GLCM based Feature Extraction Method . . . . .	23
4.4	Convolution Neural Network . . . . .	27
4.5	Internal defect: Translucent content and Yellow gummy latex . . . . .	27
4.5.1	Short Wavelength Near Infrared (SW-NIR) Region . . . . .	28
4.6	AS7263 NIR Sensor . . . . .	29
4.6.1	Optical Filters . . . . .	30
4.6.2	Multi-spectral sensing and Calibration . . . . .	30
4.6.3	Spectral data collection . . . . .	30
4.7	Feature Selection . . . . .	31
4.7.1	Statistical Significance Analysis . . . . .	31
4.7.2	Principal Component Analysis . . . . .	32
4.8	Classification Tasks . . . . .	33
4.8.1	Surface Roughness Classification . . . . .	33
4.8.2	Internal defects classification . . . . .	33
4.8.3	Machine Learning Approach . . . . .	33
4.8.4	Random Forest . . . . .	34
4.8.5	Support Vector Machine . . . . .	34
4.8.6	Performance Evaluation . . . . .	35
4.9	Development Environment . . . . .	35
<b>5</b>	<b>Experiments and Results</b>	<b>37</b>
5.1	Experiment 1: Surface Roughness Classification using Texture features . . . . .	37
5.1.1	Objective . . . . .	37
5.1.2	Experiment Setup . . . . .	37

5.1.3	Evaluation Models . . . . .	39
5.1.4	Results . . . . .	39
5.2	Experiment 2: Surface Roughness Classification using Deep learning . . . . .	40
5.2.1	Objective . . . . .	40
5.2.2	Experiment Setup . . . . .	40
5.2.3	Evaluation Models . . . . .	40
5.3	Results . . . . .	41
5.4	Experiment 3: Internal Defect Classification using NIRS Spectrum . . . . .	42
5.4.1	Objective . . . . .	42
5.4.2	Experiment Setup . . . . .	42
5.4.3	Reflection Spectral Analysis . . . . .	43
5.4.4	Evaluation Model . . . . .	44
5.4.5	Results . . . . .	44
<b>6</b>	<b>Discussion</b>	<b>46</b>
<b>7</b>	<b>Conclusion</b>	<b>48</b>
7.0.1	Limitations and Future Work . . . . .	48
	<b>Bibliography</b>	<b>50</b>

# List of Figures

1.1	System overview of proposed method. . . . .	4
2.1	Schematic diagram of proposed curvelet based fruit grading method. [9] . . . . .	7
2.2	Different sample of oranges used for this work. From left to right and top to bottom: two normal oranges, an orange with several surface defects, a morphology defect, an orange with color defect, and an orange affected by a black mould. [10] . . . . .	8
2.3	(2.3a) Image acquisition, Two classes of mangosteen surface: (2.3b) Fine, (2.3c) Defect. [7] . . . . .	9
2.4	Three configurations of spectral acquisition with variation in relative position of light source to detector and orientation of stem–calyx axis of the fruit. L135FH: Light source is 135° to the detector with fruit stem–calyx axis horizontal. L135FV: Light source is 135° to the detector with fruit stem–calyx axis at 90° to the light direction. L90FH: Light source is 90° to the detector with fruit stem–calyx axis horizontal. [24] . . . . .	12
2.5	Average absorbance of light transmitted through normal and translucent mangos- teens as affected by different fruit orientation and position of light source relative to detector. [24] . . . . .	12
3.1	Resolution cells 1 and 5 are 0°(horizontal) nearest neighbors to resolution cell *; resolution cells 2 and 6 are 135°nearest neighbors; resolution cells 3 and 7 are 90°nearest neighbors; and resolution cells 4 and 8 are 45°nearest neighbors to *. [26]	14
3.2	Architecture of Convolutional neural network. [27] . . . . .	15
3.3	NIR in the electromagnetic spectrum. [28] . . . . .	16

3.4	An infrared spectrum can be obtained by passing infrared light through a sample (transmission) or the light can be reflected from the sample (reflectance). [29] . . .	17
3.5	AS7263 Block diagram. [30] . . . . .	18
4.1	External defects:(4.1a) Glossy surface, (4.1b) Medium rough surface, (4.1c)Extreme rough surface, . . . . .	20
4.2	Region of interest obtained by cropping mangosteen images: (4.2a) Glossy surface, (4.2b) Medium rough surface, (4.2c)Extreme rough surface . . . . .	22
4.3	Directions for generation of GLCM. [31] . . . . .	23
4.4	Texture feature extraction using GLCM. . . . .	24
4.5	Classes of Internal Defects:(4.5a)Normal, (4.5b) Translucent content and (4.5c) Yellow gummy latex. . . . .	28
4.6	The ams NIR AS7263 sensor showing integration of multichannel spectral sensors.	29
4.7	Data reading from serial port . . . . .	31
4.8	Hyperplanes for linearly seperable data . . . . .	35
4.9	Confusion Matrix for two-class three-class classification model. . . . .	36
5.1	Correlation heatmap of texture feature dataset . . . . .	39
5.2	(5.2a) Training Vs Validation accuracy of Simple CNN with Adam optimizer, (5.2b) Training Vs Validation accuracy of Resnet50 with Adam optimizer. . . . .	41
5.3	(5.3a) Training Vs Validation accuracy of Simple CNN with Adamax optimizer, (5.3b) Training Vs Validation accuracy of Resnet50 with Adamax optimizer. . . .	42
5.4	NIRS data reading (5.4a) Four sides of a sample numbered through calyx, (5.4b) Sample placed close to light source for NIRS data collection. . . . .	44
5.5	Reflectance spectra of 3 classes of mangosteen sample in 6-channels of NIR wavelength at 610, 680, 730, 780, 810 and 860 nanometer (nm) respectively. . . . .	45

# List of Tables

2.1	The result of classification with percentage accuracy . . . . .	8
4.1	Surface roughness class description . . . . .	20
4.2	Description of simple CNN layers. . . . .	27
4.3	Internal defects class description . . . . .	28
4.4	Comparison results of the extracted features. . . . .	32
5.1	Details of surface roughness classification dataset . . . . .	38
5.2	Details of Principal components . . . . .	38
5.3	The comparison of accuracy between SVM and RF with and without PCA . . . . .	40
5.4	The Comparison of accuracy between Simple CNN and Resnet50. . . . .	41
5.5	Attributes indicated by 6 channels in NIR wavelength and three classes for internal defect classification. . . . .	43
5.6	The Comparison of accuracy between variants of SVM . . . . .	45

# Chapter 1

## Introduction

### 1.1 Background

The purple Mangosteen (*Garcinia mangostana*) is considered one of the well-known tropical fruits grown in South East Asia. It is one of the fruits that has an enormous export potential in Thailand. It is well-known as the queen of fruit. For Thailand, this fruit export revenue hits almost 64 million USD in 2011 [1]. The fruit mangosteen and its export has great potential to contribute to the country's economy and to many people involved in the middle like farmers, wholesaler, retailer. To improvise quality grading of fruit and maximize the export is the major concern. Currently the problem faced by mangosteens gardeners/exporters is that there is still a lack of accurate and practical non-destructive inspection technology to assure the irregular quality of the Mangosteen.

In order to fully grasp the benefits of Mangosteen export, consumer satisfaction based on the fruit quality must be considered. Apart from the traditional method of quality assurance, automated system would contribute to enhance the fruits quality assurance.

### 1.2 Problem Descriptions

With its revenue generating capability, popularity among the local consumer and in the international market there comes a challenge of quality assurance. The major problem related to the export of mangosteen is quality assurance and damage control during preharvest and postharvest phase.

Postharvest damage in fresh mangosteens at wholesale level in Thailand was investigated from

April to October 2004. A total of 37.1 % of the production yield was rendered inedible by damage during this period; damages included fruit cracking, hardened rinds, rough surfaces, translucent flesh, gummosis and decay [2]. Mangosteen like any other fruit contains many undesirable external as well as internal condition which results in the shipment rejection and decrease the reliability of the export. Fruit quality is ascertained by observing not only external factors including color, shape, size, skin blemishes, latex staining, and insect damage but also internal factors such as translucency of the flesh, the yellow gummy latex, and the hardening pericarp. These factors appreciably influence consumer acceptance [3].

These problems and defects of the fruit need to be addressed so as to minimize the shipment rejection and maximize the reliability of the export. However, the traditional process of mangosteen grading for export purposes requires expertise from gardeners with long experience. Export cannot be relied upon just the inspection from human expertise as it might not be practical for large scale exports and there are always high chances of inaccurate results. To make large scale export of mangosteen more reliable and hence to generate more revenues automated quality assurance based on Image processing, computer vision and Near infrared spectroscopy for non-destructive grading of the fruit has huge prospects.

### **1.3 Research Objectives**

As discussed in the problem description section, mangosteen has several internal and external defects. This research aims to investigate non-destructive approach for quality grading of mangosteen with the application of image processing and near infrared spectroscopy. Surface roughness detection and classification based on texture features analysis and deep learning is done. This research also aims to address two major internal defects known as translucent content and yellow gummy latex in Mangosteen by means of near infrared spectroscopy. In this study, for the first time, we propose the textural features extracted using Gray-Level Co-occurrence Matrix (GLCM) for surface roughness classification of Mangosteen into the following 3 classes:

- Glossy Surface (GS)
- Mid Rough Surface (MR) and

- Extreme Rough Surface (ER)

Along with hand crafted textural features we will compare the classification of surface roughness based on self learned features using convolution neural network which is the framework of deep learning.

With the application of Near Infrared Spectroscopy we want to classify mangosteen sample as:

- Normal sample (NS)
- Translucent defect sample (TD)
- Yellow gummy latex sample (YG)

We propose the application of both Image processing and Near Infrared Spectroscopy to address both internal and external quality grading of mangosteen. For each mangosteen sample in our study we will address its surface roughness as external defect and the presence of translucent content and yellow gummy latex as internal defect.

## **1.4 Scope**

This study is outlined as shown in figure 1.1 It uses collection of mangosteen samples for image processing and spectral data acquisition.

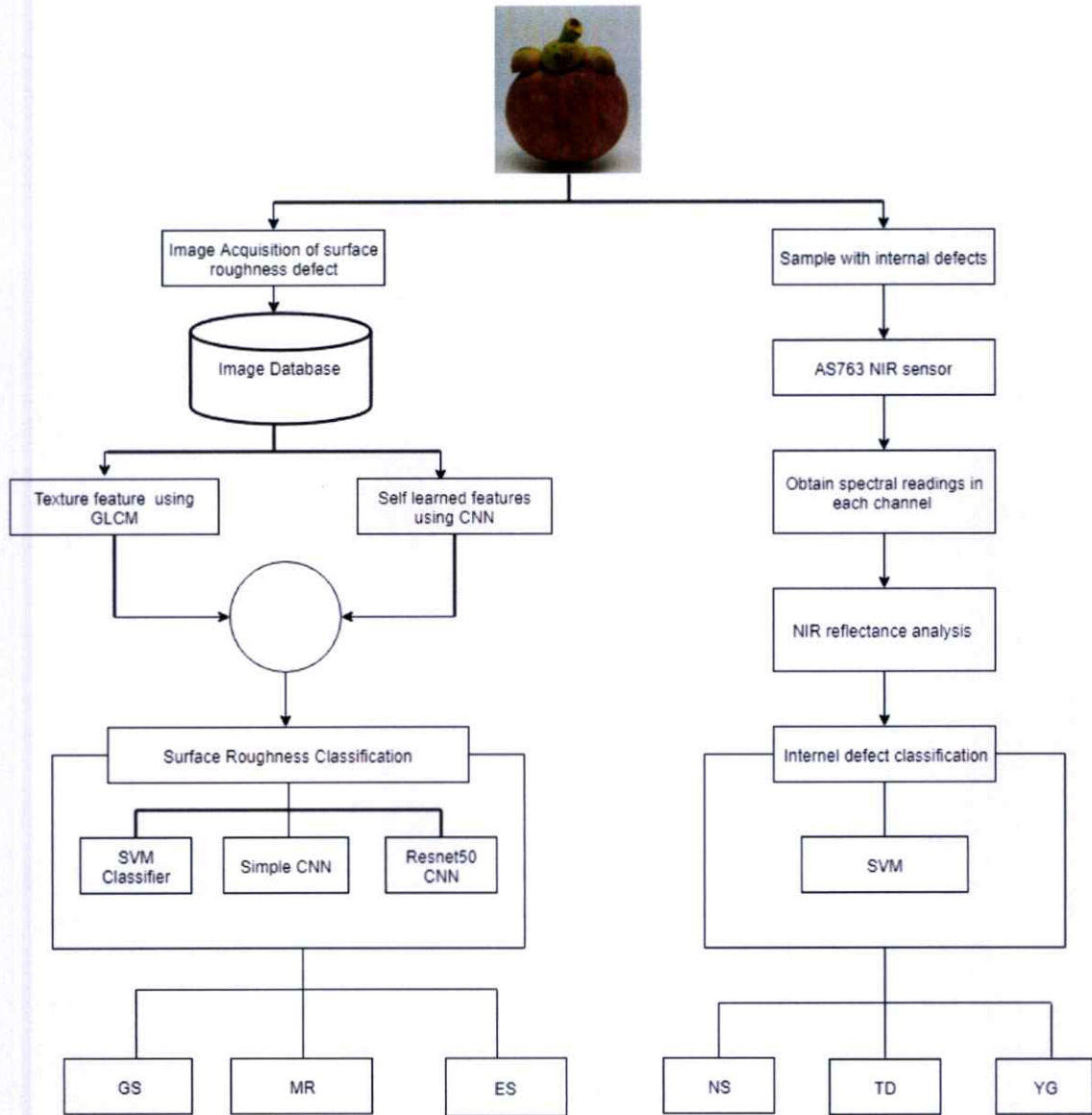


Figure 1.1: System overview of proposed method.

# Chapter 2

## Literature Review

This chapter is devoted for literature review, which includes past studies, related works and theories that involve in this research. Detailed information can be found in following sections.

### 2.1 Computer vision and Image processing

Computer vision and image processing work together in many cases. Many computer vision systems rely on image processing algorithms. Most of the time we see that computer vision and image processing are considered interchangeable terms. They both involve doing some computations on images. Both of them use image as input but image processing deals with transformation like detecting edges, smoothness, contrast, brightness etc. and its output is also image. Whereas computer vision is inclined towards what machine sees and outputs task-specific knowledge, such as object detection, object labeling and coordinates.

### 2.2 Texture Analysis

An image texture is a set of metrics calculated in image processing designed to quantify the perceived texture of an image. Texture analysis refers to the characterization of regions in an image by their texture content. Texture is one of the most important features in computer vision for many applications. It has prospects in various applications, which includes remote sensing, automated inspection, and medical image processing. Major challenge in texture analysis is to obtain parame-

ters that describes the texture of an image. There are many algorithms for texture feature extraction from digital images.

## **2.3 Surface defect detection of fruits**

The surface defect detection of fruits is a challenging task, which influences market value and consumer preferences to purchase fruits. The early detection of fruit surface defects is a significant task in packing houses because a defected fruit can spread the infection such as fungal growth, bruises to other fruits, which are packed in the batch [4]. For the surface defect detection of fruits from digital images many techniques have been developed so far.

Looking back to the study of the image texture feature extraction process in the past 50 years, lots of progress has been made. Extraction of image texture feature is usually a key process in image texture description, classification and segmentation. Many different methods and algorithms are put forward for this purpose, for example, the GLCM method, the gray level run length method and auto correlative function method [5]. Texture analysis is important in many applications of computer image analysis for classification or segmentation of images based on local spatial variations of intensity or color. Textures are characteristic intensity variations that typically originate from roughness of object surfaces. Generally, it can be defined as a regular repetition of elements or pattern on a surface. These texture images vary in brightness, color, shape, size, etc [6].

Many results are published, in which image processing is used to assess some particular quality features based on color, texture and morphology in fruit grading. Image processing techniques have been widely used for surface inspection and grading of of fruits. Machine vision systems for visual sizing and color are fairly used in the food processing industry. The surface defects or diseases appearing on the fruits are characterized by different texture patterns [7]. Machine vision system with effective image processing methods are used in quality grading of agricultural products. A pattern recognition technique was developed to detect and classify surface defects such as pitting, splitting and stem-end rot found in images of mandarin fruits. The developed technique employs fuzzy thresholding for image segmentation, binary wavelet transform (BWT) for feature extraction and a rule based linear classifier model for detection and classification of the defects [8]. Suchitra A. Khoje developed an evaluation methodology for quality of fruit surfaces. The objective of this

approach was to develop a methodology for assessing fruit quality using texture analysis based on Curvelet Transform. Image acquisition of fruit sample was done using a CCD color camera. Guava and lemon were two fruits analyzed in the experiment. Textural measures based on curvelet transform such as energy, entropy, mean and standard deviation were used to characterize fruits' surface texture. These textural information is combined using classifiers to recognize defected fruits from healthy one. These four extracted features are independently tested on two classifiers, Support Vector Machines (SVM) and Probabilistic Neural Networks (PNN). Overall classification rates achieved with these classifiers for combined features range from 89 to 91 % [9] .

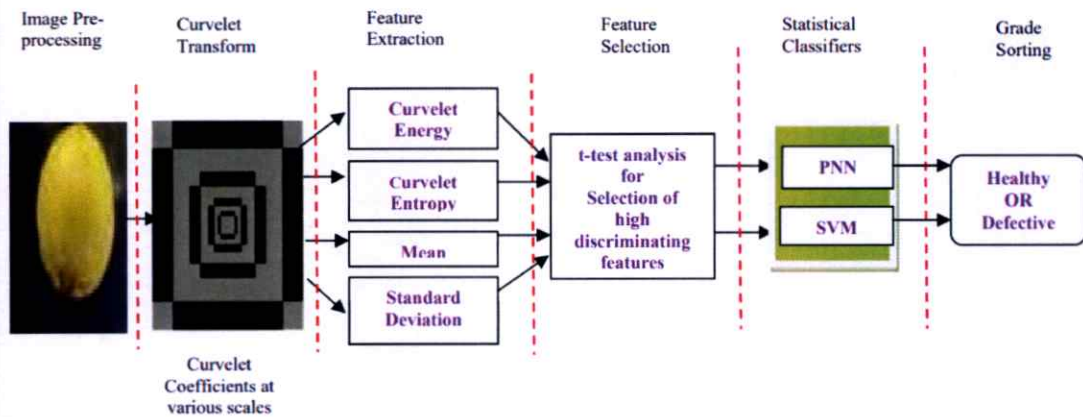


Figure 2.1: Schematic diagram of proposed curvelet based fruit grading method. [9]

[10] have developed an approach for fruit surface defect classification with color and texture features. The texture and gray features of defect area are extracted using gray level co-occurrence matrix and classification is performed using RBPNN. The proposed technique is very robust and can identify specific defects like: surface defect, morphological defect, color defect, black mould or recognize a normal fruit as shown in figure 2.2.

[11] use wavelet packet transform based image processing algorithm for the classification of external defects in citrus fruit. Defects included pitting, splitting and stem-end rot. The mean and standard deviation calculated for the detail as well as the approximation sub-windows of the wavelet packet transformed images of the citrus fruits were used as features with neural network classifier. [1] presented non-destructive approach for mangosteen grading which was based on external features like color texture, calyx, flaw, shape and size of mangosteen. Mangosteen is classified into extra class, class I and class II based on these features. Surface defects like bruises and roughness

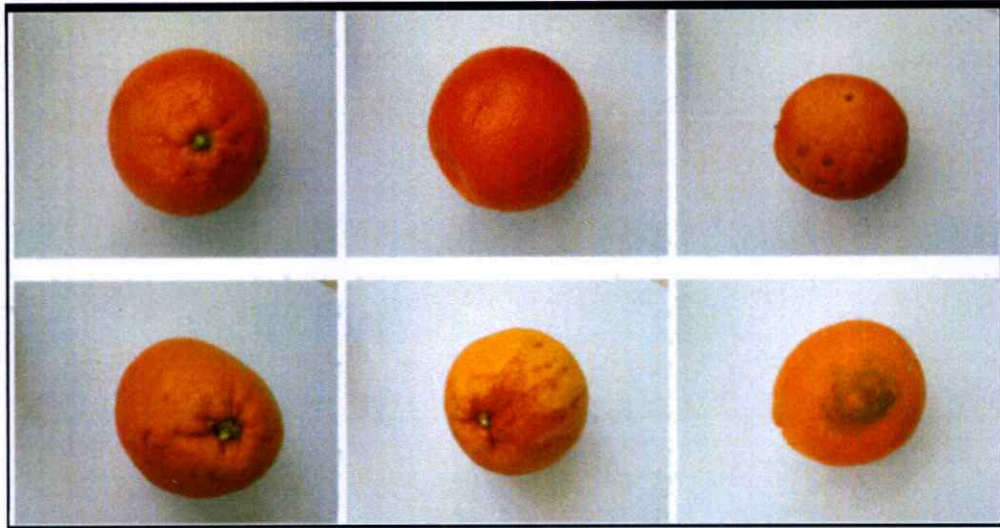
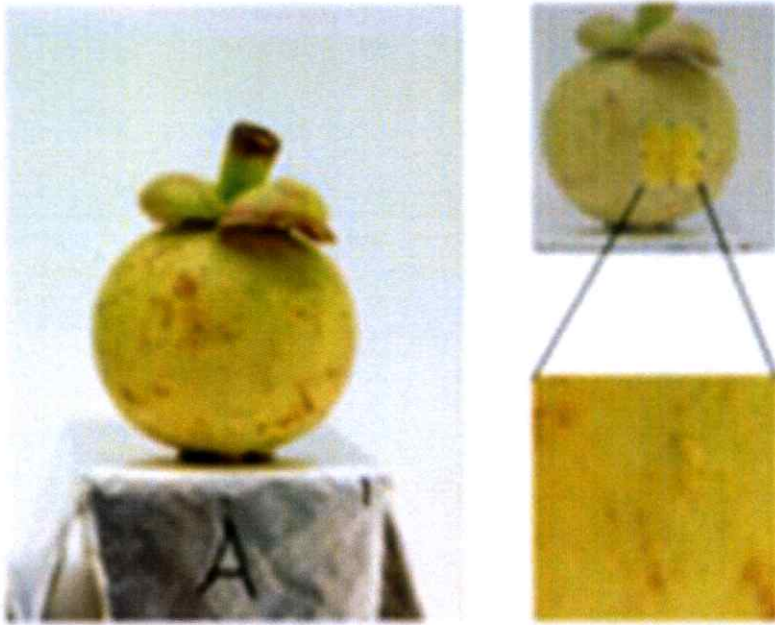


Figure 2.2: Different sample of oranges used for this work. From left to right and top to bottom: two normal oranges, an orange with several surface defects, a morphology defect, an orange with color defect, and an orange affected by a black mould. [10]

hinders export potential. A research was done by Damarjati et al in paper entitled Evaluation of Mangosteen Surface Quality using Discrete Curvelet Transform (DCT). This study incorporates pre-processing, implementation of DCT, statistical features extraction and classification using linear discriminant analysis [12]. [7] Yet another research paper from Damarjati et al. tried to solve the issue of mangosteen defect classification using one of deep learning architecture that is Convolutional Neural Network (CNN). First mangosteen sample is sorted by expert as defective and defect free. They have two classes of surface defect labelled as “fine” and “defect” as shown in figure 2.3b and 2.3c respectively. The results of the experiments using CNN algorithm showed the performance of defect detection on the mangosteen fruit of 97% as seen in Table 2.1.

Table 2.1: The result of classification with percentage accuracy

Algorithm	Percentage Accuracy (%)				Mean
	fold-1	fold-2	fold-3	fold-4	
CNN	100	100	93.33	96.67	97.5



(a)



(b)



(c)

Figure 2.3: (2.3a) Image acquisition, Two classes of mangosteen surface: (2.3b) Fine, (2.3c) Defect.  
[7]

## 2.4 Internal defects of Mangosteen

Internal factors such as translucent flesh and yellow gummy latex are major constraint to export of mangosteen. Various destructive and non-destructive approach has been developed for estimation of internal defects in mangosteen. Pankasemsuk (1996) used the floating technique by using differences in specific gravity is non-destructive detection of translucent fresh disorder in mangosteen [13]. Furthermore, the microwave technique used to classify the mangosteen with a translucent fresh disorder out from the good one finding of a threshold in term of magnitude of the reflect microwave signal through a mangosteen, the monopole probe is chosen [14]. Rittisak proposed the resonance frequency measurement to detect translucent fresh disorder and yellow gummy latex in mangosteen fruit [15]. Several nondestructive methods based on X-ray and nuclear magnetic resonance (NMR) have been studied for internal quality evaluation of fruits and vegetables. Yantarasri proposed a method using X-ray and NMR for non-destructive internal quality evaluation of durian and mangosteen [16]. Mansyah et al. (2003) reported that yellow latex on the exocarp correlated positively to temperature, days of rain, total rainfall, and leaf K content. Yellow latex in the endocarp was positively correlated with rainfall and relative humidity in which the higher the rainfall and relative humidity, the higher the percentage of fruit with yellow latex in the endocarp [17]. Both translucent flesh and yellow gummy latex seems to be caused by excessive water absorption during flowering to harvest period.

### 2.4.1 Near Infrared Spectroscopy

Near infrared (NIR) spectroscopy (NIRS) is a type of high-energy vibrational spectroscopy performed in the wavelength range from 750 to 2500 nm. NIR is gaining popularity in food industry as an analysis toll. NIR spectra contains information about all the molecules containing hydrogen thereby enabling a humungous scope of organic compound analysis. NIRS is a non-destructive practical method with reliable reproducibility in results that can replace expensive, time consuming and labor intensive methods that are in practice for customary validation in food industry [18].

(NIRS) is known as a rapid technique to evaluate the quality traits of fruits and vegetables. Many researches related to the methods for implementation of NIRS has been successfully published and some are ongoing. There are several advantages of NIRS compared to some traditional

chemical methods like fast speed, accuracy, minimal sample preparation, no use of toxic reagents, fast processing and result etc.

NIRS has been proven to be a very useful technique for non-destructive classification of diverse intact fruit [19]. An increasing number of researchers have concentrated on transmission spectra as NIR diffuse reflectance spectra are only able to acquire data approximately one centimeter into the intact sample [20]. Many researchers have investigated the use of short wavelength near infrared (SW-NIR) spectroscopy based on the transmittance mode for an accurate evaluation of the internal quality of fruit [21]. To detect hidden internal disorders in intact fruit, NIR instruments which comprise a transmission mode are required for light to be able to sufficiently penetrate the fruit [22]. Watercore disorder in apple was quantified with high levels of accuracy with the application of light transmittance intensity in the range of 760–810 nm [23]. Translucent disorder in mangosteen is accompanied by significantly higher water content in pericarp and flesh than normal fleshy fruits. Translucent flesh disorder is undesirable in mangosteen meant for export. Mangosteen fruit with translucency visible on the flesh surface may contain an identical amount of translucent content as that of fruit considered to be normal (that is, with no apparent translucency on the flesh surface) [24]. Internal translucency is important to be determined and thus the demand of nondestructive technique which can predict translucent content is growing.

Anupun et al. developed a non-destructive model to estimate the translucent content in mangosteen using near infrared transmittance spectroscopy. In their experiment they take into consideration of the effects of fruit orientation and the position of light source while taking spectral measurement.

The spectra of both the normal and translucent fruit were averaged for three dissimilar configurations. Negative absorbance was noticeable at wavelengths around 815 nm for the translucent fruit. The translucent flesh, which had higher water content, transmitted more light than the normal flesh.

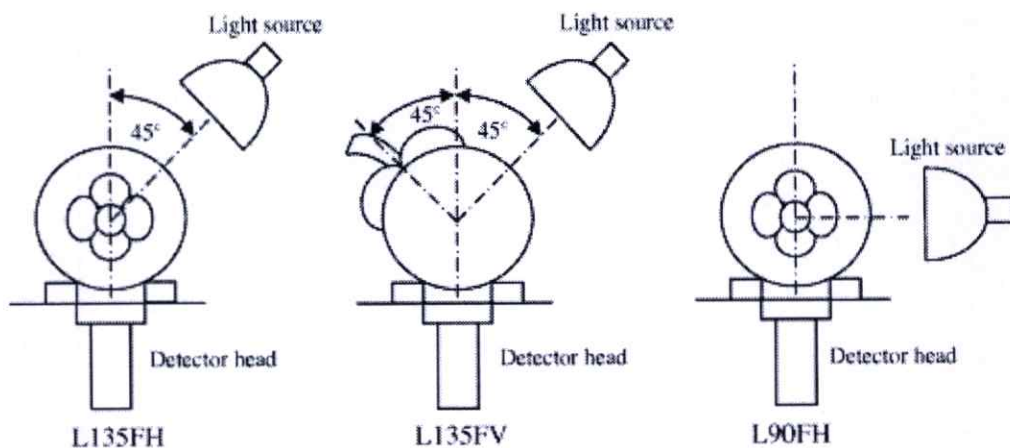


Figure 2.4: Three configurations of spectral acquisition with variation in relative position of light source to detector and orientation of stem–calyx axis of the fruit. L135FH: Light source is 135° to the detector with fruit stem–calyx axis horizontal. L135FV: Light source is 135° to the detector with fruit stem–calyx axis at 90° to the light direction. L90FH: Light source is 90° to the detector with fruit stem–calyx axis horizontal. [24]

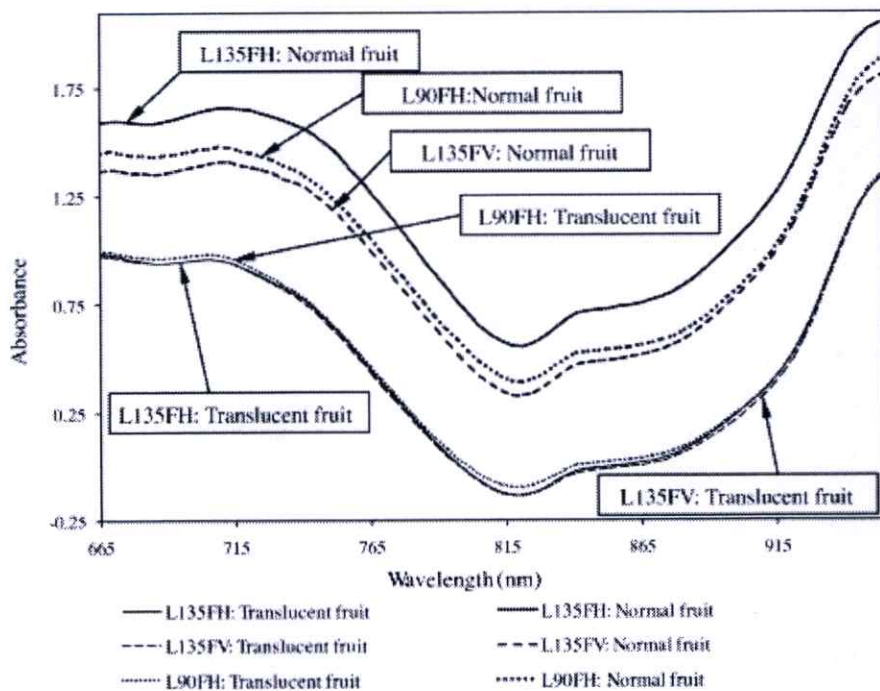


Figure 2.5: Average absorbance of light transmitted through normal and translucent mangosteens as affected by different fruit orientation and position of light source relative to detector. [24]

# Chapter 3

## Background Knowledge

This chapter introduces various notions and concepts that is used in this research. Concise explanation, including fundamental information, will be pointed out.

### 3.1 Mangosteen

Mangosteen (*Garcinia mangostana*) is a tropical fruit native to South East Asia and contains various active compounds with putative health effects [25]. Grading is essential for marketing because pricing is tied to produce quality. Quality sorting criteria of fresh mangosteens include size, color and defects [2].

Rough surface is one of the major external defects which has impact on consumer preference. Translucent flesh and yellow gummy latex are two major internal defects which results due to excess water content in the flesh. Translucent flesh occur because of excessive absorption of moisture either from roots, leaves or the fruit.

### 3.2 Gray Level Co-occurrence Matrix

Gray level co-occurrence matrix (GLCM) was suggested by Haralick et al [26]. It is one of the widely used texture analysis algorithm. Spectral, textural, and contextual features are three fundamental pattern elements used in human interpretation of color photographs. Haralick et al presents a general procedure for extracting textural properties of blocks of image data. These features are

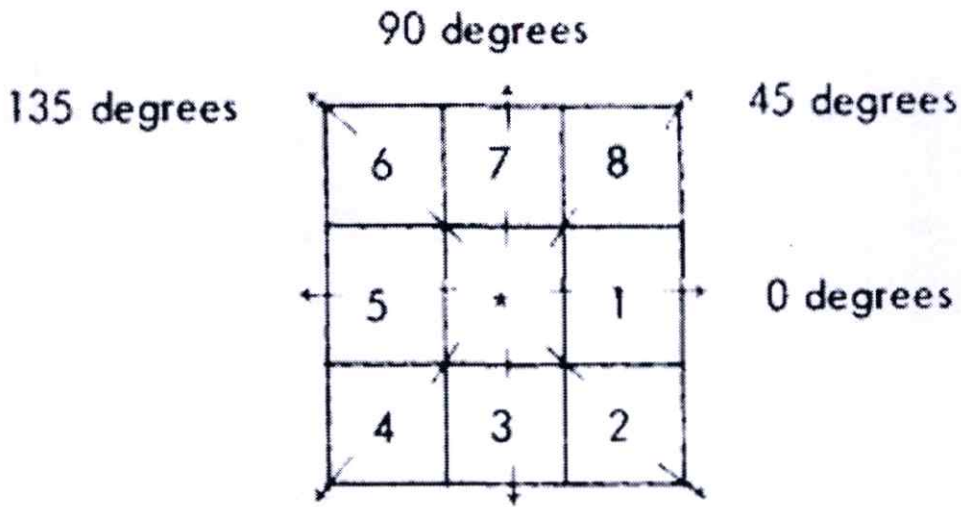


Figure 3.1: Resolution cells 1 and 5 are 0°(horizontal) nearest neighbors to resolution cell \*; resolution cells 2 and 6 are 135°nearest neighbors; resolution cells 3 and 7 are 90°nearest neighbors; and resolution cells 4 and 8 are 45°nearest neighbors to \*. [26]

calculated in the spatial domain, and the statistical nature of texture is taken into account, which is based on the assumption that the texture information in an image  $I$  is contained in the overall or "average" spatial relationship which the gray tones in the image have to one another. A set of graytone spatial-dependence probability-distribution matrices is computed for a given image block and suggest a set of 14 textural features which can be extracted from each of these matrices. These features contain information about such image textural characteristics as homogeneity, gray-tone linear dependencies (linear structure), contrast, number and nature of boundaries present, and the complexity of the image. Suppose an image to be analyzed is rectangular and has  $N_x$  resolution cells in the horizontal direction and  $N_y$  resolution cells in the vertical direction. We consider a resolution cell-excluding those on the periphery of an image, etc. to have eight nearest-neighbor resolution cells as in Figure 3.1

Let  $L_x = \{1, 2, \dots, N_x\}$  be the horizontal spatial domain,  $L_y = \{1, 2, \dots, N_y\}$  be the vertical spatial domain, and  $G = \{1, 2, \dots, N_g\}$  be the set of  $N_g$  quantized gray tones. The set  $L_y * L_x$  is the set of resolution cells of the image ordered by their row-column designations. The image  $I$  can be represented as a function which assigns some gray tone in  $G$  to each resolution cell or pair of coordinates in  $L_y * L_x$ ;  $I : L_y * L_x \rightarrow G$ . We assume that the texture-context information in an image  $I$  is contained in the overall or "average" spatial relationship which the gray tones in image

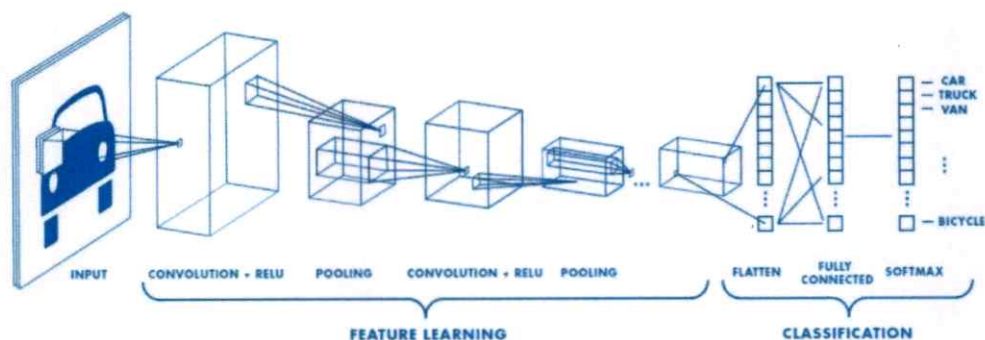


Figure 3.2: Architecture of Convolutional neural network. [27]

I have to one another. Texture-context information is adequately specified by the matrix of relative frequencies  $P_{ij}$  with which two neighboring resolution cells separated by distance  $d$  occur on the image, one with gray tone  $i$  and the other with gray tone  $j$  [26].

### 3.3 Deep Learning

Deep learning is a machine learning technique that teaches computers to do what comes naturally to humans: learn by example. In deep learning, a computer model learns to perform classification tasks directly from images, text, or sound. Deep learning models can achieve state-of-the-art accuracy, sometimes exceeding human-level performance.

#### 3.3.1 Convolution Neural Network

It is one of the most popular type of deep neural network commonly called as CNN or ConvNet. A CNN convolves learned features with input data and eliminates need for manual feature extraction. The CNN works by extracting features directly from images. [27] The general architecture of CNN can be depicted as shown in fig. 3.2.

#### 3.3.2 Transfer Learning

Conventional machine learning and deep learning algorithms are designed in traditional approach and they work in isolation. In the beginning these algorithms are trained with some datasets to perform specific tasks. Later if we want to use the same model for slightly different datasets,

# NIR in the Electromagnetic Spectrum

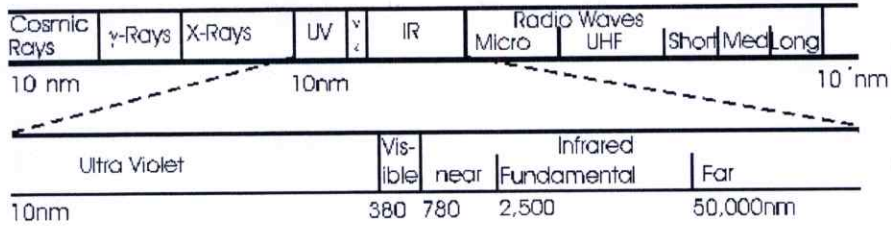


Figure 3.3: NIR in the electromagnetic spectrum. [28]

we need to rebuild the model and retrain the algorithms. So Transfer learning is the new concept which overcomes the isolated learning paradigm and provide the possibilities of utilizing knowledge acquired for one task to solve related ones.

## 3.4 Near Infrared Spectroscopy

Near-infrared spectroscopy (NIRS) is a spectroscopic method that uses the near-infrared region of the electromagnetic spectrum (from 780 nm to 2500 nm). Spectroscopy is defined as the interaction between light and matter. Near Infrared is an accurate and rapid analysis method that is well suited for quantitative determination of the major constituents in most types of food and agricultural products and in medical diagnosis. In figure 3.3 we can see near infrared region in the electromagnetic spectrum [28].

### 3.4.1 Working Principle

Two commonly heard terms in connection with NIR are 'reflectance' and 'transmission'. Let's take a look at what they are about Near Infrared light is directed onto a sample The light is modified according to the composition of the sample. Mmodification could be reflection, absorption or transmission and this modified light is detected The spectral modifications are potential source of information regarding the composition of the sample. Figure 3.4 shows working principle of NIR absorption and reflection spectrum [29].

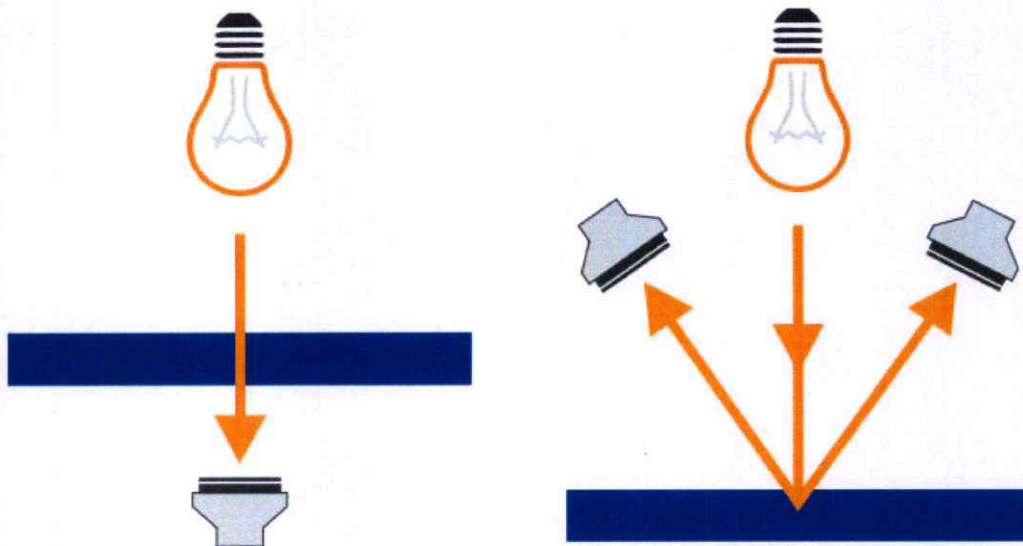


Figure 3.4: An infrared spectrum can be obtained by passing infrared light through a sample (transmission) or the light can be reflected from the sample (reflectance). [29]

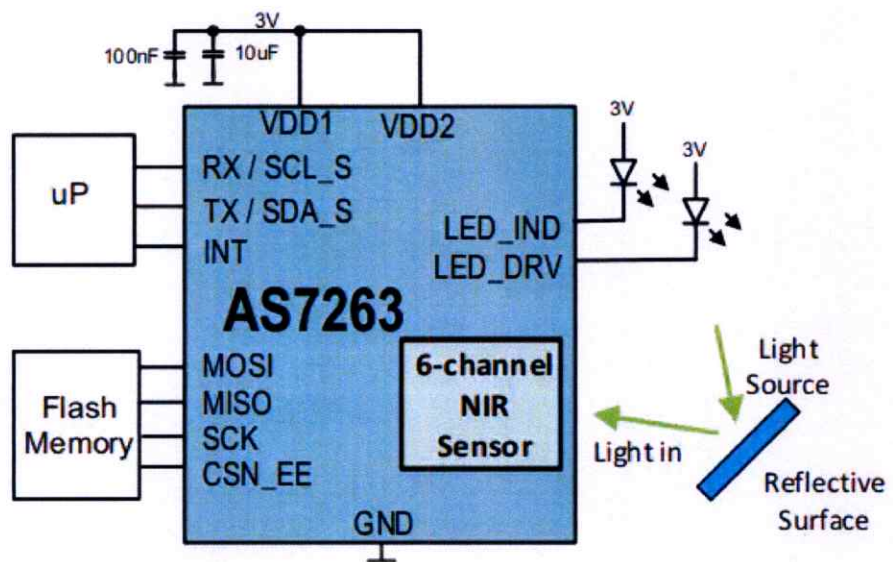
### 3.4.2 NIR Sensors

There are many portable pocket sized or hand-held infrared devices. Development of such devices or spectra sensors has brought the spectroscopy to the palm of our hand. These sensors are low cost and can be used in a wide variety of material sensing applications.

### 3.4.3 AS7263 NIR Sensor

The AS7263 is a digital 6-channel spectrometer for spectral identification in the near IR (NIR) light wavelengths [30]. It measures spectrum from reflections. AS7263 consists of 6 independent optical filters whose spectral response is defined in the NIR wavelengths. Figure 3.5 shows the block diagram of AS7263 nir sensor. The AS7263 spectrometer detects wavelengths in the range at 610, 680, 730, 760, 810 and 860nm of light each with 20nm of full-width half-max detection.

The AS7263 sensor is combined with Gaussian filters into standard CMOS silicon via Nano-optic deposited interference filter technology and is packaged in an LGA package which provides an aperture to control the light entering the sensor array. It can communicate using both an I<sup>2</sup>C interface and serial interface using AT commands. Its usb can be used to interface directly with the computer and display the spectral data from the sensor with a baud rate of 115200.



76

Figure 3.5: AS7263 Block diagram. [30]

# Chapter 4

## Methodology

This chapter introduces proposed methods and flow of the task in this study. The first section is Data collection with the detail explanation of our approach of collecting mangosteen sample. Second section, Gray Level Co-occurrence Matrix , will explain about the architecture of co-occurrence matrix and about the textural features that can be extracted from the co-occurrence matrix. Third section discuss about convolutional neural network with details about each layer which is used in our experiment. The final section will explain about Near Infrared Spectroscopy.

### 4.1 Data Collection

Primary data of our research is mangosteen. We proceed with considering 3 different level of roughness which was based on expert/farmers opinion and experience. We also collected another group of sample with internal defects i.e, translucent sample and samples with yellow gummy latex. All the collected samples were brought back to laboratory from the farm for image acquisition and nir data collection.

### 4.2 External defect:surface roughness

Mangosteen is initially sorted based on surface roughness into 3 different classes as glossy surface, medium rough surface and extreme rough surface respectively. Three classes can be listed based on heuristic expert knowledge definition in Table 4.1.



(a)



(b)



(c)

Figure 4.1: External defects:(4.1a) Glossy surface, (4.1b) Medium rough surface, (4.1c)Extreme rough surface,

Table 4.1: Surface roughness class description

Surface Class	Description
Glossy (GS)	Fine smooth surface with very minimum or no skin bruises. This class gets more consumer's preference and pricing is highest.
Medium Rough (MR)	Coarse surface. This class gets lower consumer's preference and pricing lower to glossy. Acceptable for export.
Extreme Rough (ER)	Degree of coarseness is higher than medium rough class. Unpleasant to touch, lower consumer acceptance and mainly sold in local markets. Not for export.

### **4.2.1 Image Acquisition and Pre-processing**

Mangosteen is initially sorted based on roughness into 3 different classes by experts/farmers. For the same sample image was acquired using camera and UDIO Lighting Studio Box. Sample was placed inside the UDIO box and image was captured by rotating sample clockwise and facing each calyx . In this way we captured four images per sample.

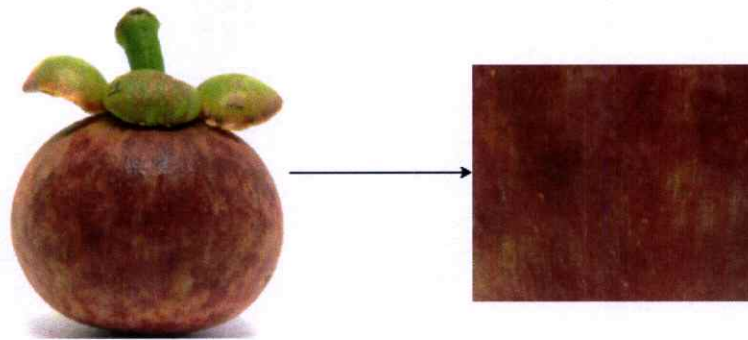
Digital images are prone to various types of noise which might have resulted from our flaws during image acquisition process. Such noise reduces the quality of our image and lead to inaccurate results. We attempt to remove noise from our data using Median filter. And for these image samples we compute gray level co-occurrence matrix and then extract texture features based on the co-occurrence matrix.

### **4.2.2 Region Of Interest**

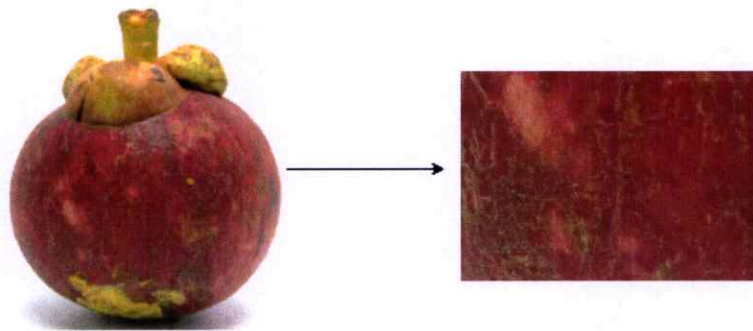
After image were captured and median filtering was done region of interest (ROI) was obtained with manual cropping. In figure 4.2 we can see image sample cropped to obtain region of interest for each class of Mangosteen.

## **4.3 Gray Level Co-occurrence Matrix**

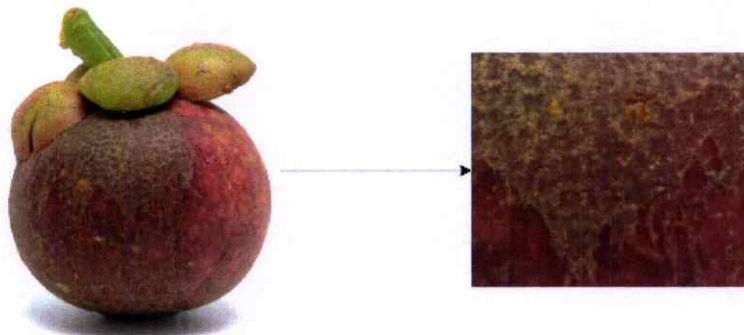
Gray level co-occurrence matrix (GLCM) was suggested by Haralick et al [26]. It is one of the widely used texture analysis algorithm. Haralick et al presents a general procedure for extracting textural properties of blocks of image data. These features are calculated in the spatial domain, and the statistical nature of texture is taken into account , which is based on the assumption that the texture information in an image  $I$  is contained in the overall or "average" spatial relationship which the gray tones in the image have to one another. A set of gray tone spatial-dependence probability-distribution matrices is computed for a given image block and suggest a set of 14 textural features which can be extracted from each of these matrices.



(a)



(b)



(c)

Figure 4.2: Region of interest obtained by cropping mangosteen images: (4.2a) Glossy surface, (4.2b) Medium rough surface, (4.2c) Extreme rough surface

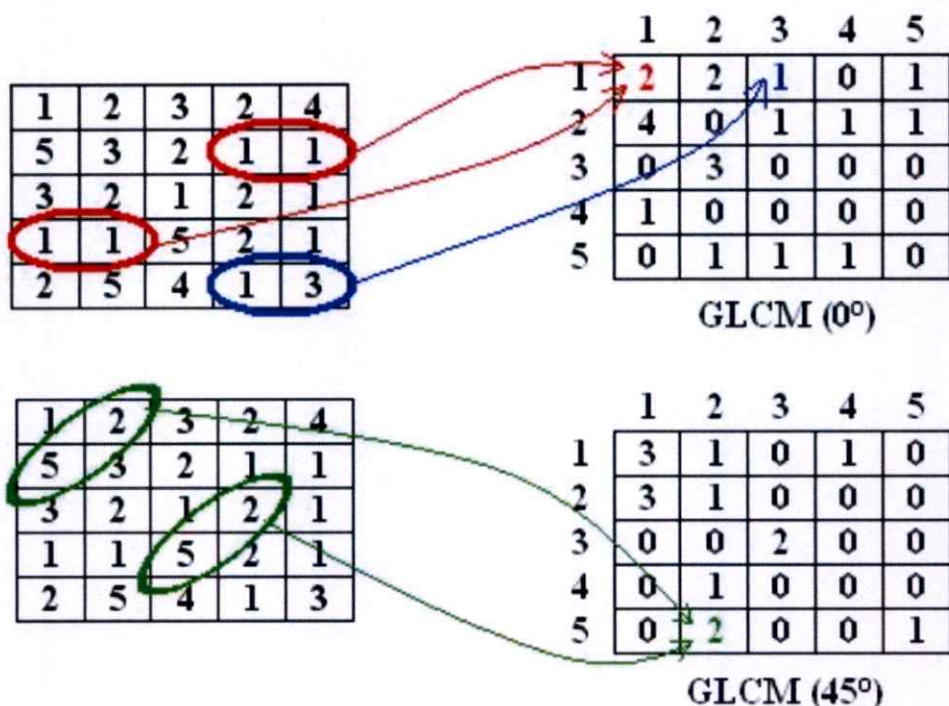


Figure 4.3: Directions for generation of GLCM. [31]

### 4.3.1 GLCM based Feature Extraction Method

Initial assumption in characterizing image texture is that all the texture information is contained in the gray-tone spatial-dependence matrices. Hence all the textural features we suggest are extracted from these gray-tone spatial-dependence matrices. Each steps in this approach is depicted in figure 4.4.

An input color image is transformed into grayscale image. In photography, computing, and colorimetry, a grayscale or grey-scale image is one in which the value of each pixel is a single sample representing only an amount of light, that is, it carries only intensity information. From figure 4.3 we can see how the co-occurrence matrix is obtained, this matrix characterizes the texture of an image by calculating how often pairs of pixel occurs [31].

For textural features of Mangosteen's surface roughness, we will be using GLCM which is a statistical method of examining texture that considers the spatial relationship of pixels [6]. All the 14 GLCM textural features suggested by Haralick et al. has been used in this work. The equations which define a set of 14 measures of textural features are given.

*Notation*

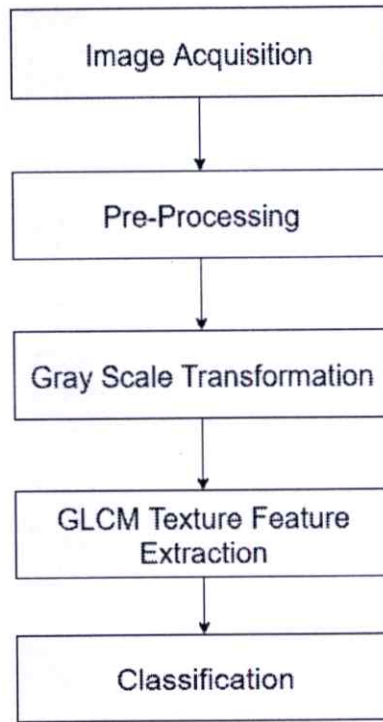


Figure 4.4: Texture feature extraction using GLCM.

$p(i, j)$   $p(i, j)$ th entry in a normalized gray-tone spatial dependence matrix,  $= P(i, j)/R$

$R$  is the normalizing constant.  $R = \sum_{i,j=1}^{N_g} P(i, j)$ .

$p_x(i)$   $i$ th entry in the marginal-probability matrix

$N_g$  Number of distinct gray levels in the quantized image. Textural Features:

1. Angular Second Moment (ASM) : Energy is also known as ASM. It measures textural uniformity of an image.

$$f_1 = \sum_i \sum_j \{p(i, j)\}^2. \quad (4.1)$$

2. Contrast : Contrast measures the quantity of local changes in an image. It reflects the sensitivity of the textures in relation to changes in the intensity. Contrast is 0 for a constant image.

$$f_2 = \sum_{n=0}^{N_g-1} n^2 \left\{ \sum_{i=1}^{N_g} \sum_{j=1}^{N_g} p(i, j) \right\}. \quad (4.2)$$

3. Correlation : This feature measures how correlated a pixel is to its neighborhood. It is the

measure of gray tone linear dependencies in the image. Feature values range from -1 to 1.

$$f_3 = \frac{\sum_{i,j} (ij) p(i,j) - \mu_x \mu_y}{\sigma_x \sigma_y} \quad (4.3)$$

where  $\mu_x$ ,  $\mu_y$ ,  $\sigma_x$  and  $\sigma_y$  are the means and standard deviations of  $p_x$  and  $p_y$

#### 4. Variance

$$f_4 = \sum_{i,j} (i - \mu)^2 p(i,j). \quad (4.4)$$

5. Inverse Difference Moment (Homogeneity) : Inverse difference moment measures image homogeneity. Homogeneity is higher when most of the occurrences in GLCM are concentrated near the main diagonal.

$$f_5 = \sum_i \sum_j \frac{1}{1 + (i - j)^2} p(i,j) \quad (4.5)$$

#### 6. Sum Average

$$f_6 = \sum_{i=2}^{2N_g} i p_{x+y}(i). \quad (4.6)$$

7. Sum Variance : It is the sum of the squares of the differences between the intensity of the central pixel and its neighbours.

$$f_7 = \sum_{i=2}^{2N_g} (i - f_6)^2 p_{x+y}(i). \quad (4.7)$$

#### 8. Sum Entropy

$$f_8 = - \sum_{i=2}^{2N_g} p_{x+y}(i) \log \{p_{x+y}(i)\}. \quad (4.8)$$

9. Entropy : Entropy is a measure of randomness of intensity image.

$$f_9 = - \sum_{i,j} p(i,j) \log(p(i,j)). \quad (4.9)$$

10. Difference Variance

$$f_{10} = \text{Var of } p_{x-y}. \quad (4.10)$$

11. Difference Entropy

$$f_{11} = - \sum_{i=0}^{N_g-1} p_{x-y}(i) \log \{p_{x-y}(i)\}. \quad (4.11)$$

12. Information Measure of Correlation I

$$f_{12} = \frac{H(X, Y) - H(X, Y)_1}{\max \{H(X), H(Y)\}}. \quad (4.12)$$

13. Information Measure of Correlation II

$$f_{13} = (1 - \exp[-2.0(H(X, Y)_2 - H(X, Y))])^{\frac{1}{2}}, \quad (4.13)$$

$$H(X, Y) = - \sum_{i,j} p(i, j) \log(p(i, j)). \quad (4.14)$$

where  $H(X)$  and  $H(Y)$  are entropies of  $p_x$  and  $p_y$ , and

$$H(X, Y)_1 = - \sum_{i,j} p(i, j) \log \{p_x(i)p_y(j)\}, \quad (4.15)$$

$$H(X, Y)_2 = - \sum_{i,j} p_x(i)p_y(j) \log \{p_x(i)p_y(j)\}. \quad (4.16)$$

14. Maximal Correlation Coefficient

$$f_{14} = (\text{Second largest eigenvalue of } Q)^{\frac{1}{2}}, \quad (4.17)$$

where

$$Q(i, j) = \sum_k \frac{p(i, k)p(j, k)}{p_x(i)p_y(k)}. \quad (4.18)$$

Table 4.2: Description of simple CNN layers.

Layer Name	Kernel size	Kernel number	Activation Function
Conv1	3*3	32	Relu
Conv2	3*3	32	Relu
Max Pooling	2*2	1	-
Conv3	3*3	64	Relu
Max Pooling	2*2	1	-
FC-1	-	-	-
FC-2	-	-	-
Output Layer	-	-	Sigmoid

## 4.4 Convolution Neural Network

Convolutional neural networks (CNN, ConvNet) is a class of deep, feed-forward artificial neural networks usually composed by a set of layers that can be grouped by their functionality. Convolutional Neural Networks consists of compound layers of networks that are basically learned through each layer. However, the data extraction grows with the level of layers [32]. These networks can extract features on their own and it is a good idea to explore their feature extraction ability and compare with hand crafted features. For utilizing deep learning for surface roughness classification we will build a cnn model and train with our image datasets from scratch. Table 4.2 shows details of CNN model that we build and train from scratch. Resnet50, a pretrained cnn model is also used for the same purpose and compare its performance with cnn model which is trained from scratch.

## 4.5 Internal defect: Translucent content and Yellow gummy latex

With the help of farmers and expert who have been working in the mangosteen export we collected samples and categorized as normal and sample with internal defects like translucent content and yellow gummy latex. Hard pericarp, irregular color development of fruit skin and presence

of yellow gum on fruit skin were the basis on which experts relied on to separate samples with translucent flesh or with gummy latex. Translucent flesh and presence of gummy latex in mangos- teen is a major cause of reduced fruit quality. Symptoms, usually found in large segments of the fruit, include flesh changes from white to translucent and textural changes from soft to firm and crisp along with yellow gum like substance. Details of internal defect class and its description is mentioned on the Table 4.3 and each class is represented by figure 4.5.

Table 4.3: Internal defects class description

Internal defect Class	Description
Normal (N)	Normal sample, white fruit pulp inside. Defect free or without gummy latex and translucent flesh.
Translucent Content (TD)	Hard pulp and looks like glass, major internal defect for export.
Yellow gummy latex (YG)	Presence of yellow gum like substance in the pericarp or fruit's flesh.



(a)



(b)



(c)

Figure 4.5: Classes of Internal Defects:(4.5a)Normal, (4.5b) Translucent content and (4.5c) Yellow gummy latex.

#### 4.5.1 Short Wavelength Near Infrared (SW-NIR) Region

Many studies in the past suggest that application of SW-NIR region 655–955 nm, is suitable for nondestructive or noninvasive analysis of fruits and vegetables. SW-NIR in both the reflection and transmission mode are used for internal defect detection like water core in fruits like apple [23]. AS7263-NIR spectrometer identifies spectra in the NIR light wavelengths in the range 610 to 860,

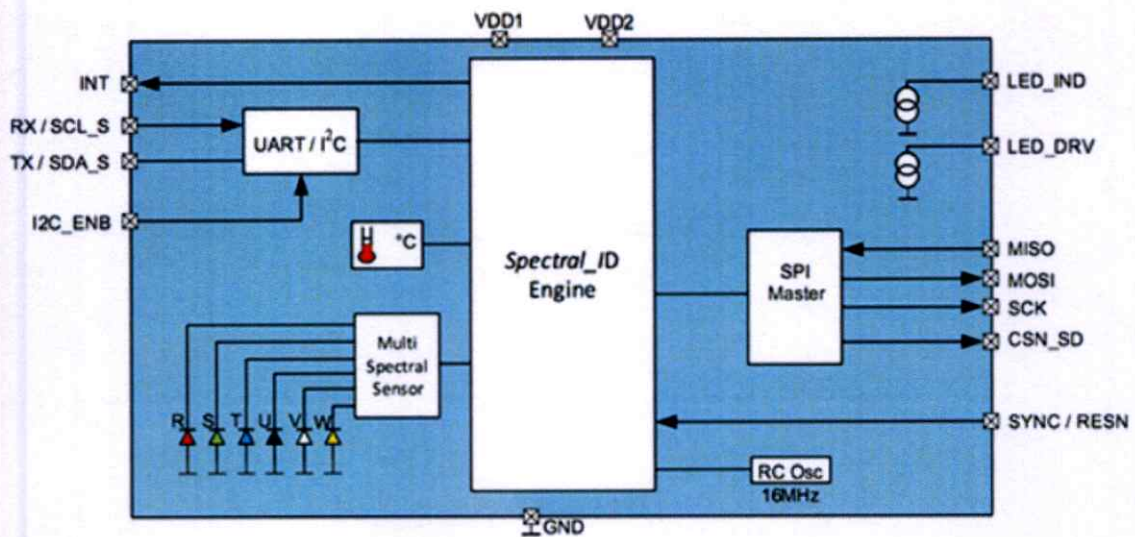


Figure 4.6: The ams NIR AS7263 sensor showing integration of multichannel spectral sensors. [30]

which includes the SW-NIR region. This sensor was our choice because of the wavelength range of SW-NIR which we were interested in for the internal quality estimation.

## 4.6 AS7263 NIR Sensor

The AS7263 is a digital 6-channel spectrometer for spectral identification in the near IR (NIR) light wavelengths. The spectrometer detects wavelengths in the range at 610, 680, 730, 760, 810 and 860nm of light each with 20nm of full-width half-max detection. It is based on reflectance spectroscopy.

The ams AS7263 IC is a complete single-chip spectrometer which integrates all essential components needed for optical spectroscopy. It also includes external LEDs to illuminate a target as seen in Figure 4.6. An integrated spectral identification (Spectral\_ID) engine processes sensor signals, which gives spectral data reading that a host MCU can access through the supported I<sup>2</sup>C/UART interface using simple commands.

## 4.6.1 Optical Filters

After illuminating a target with an appropriate light source, a reflection spectrometer uses optical filters to capture the distinct wavelengths of light that are reflected off the target [30]. The sensor consists of six independent optical filters whose spectral response is defined in the NIR wavelengths from 610 to 870 nm. Optical Filters are used to selectively transmit or reject a wavelength or range of wavelengths. As7263 NIR sensor has interference filter technology, interference filters only reflect wavelength in the NIR region and rejects other.

## 4.6.2 Multi-spectral sensing and Calibration

Ams uses a novel multi-spectral sensing design to address the reliability and ease of use of the device. Conventional semiconductor process technologies are used to build nanoscale optical interference filters. These filters are build directly on the silicon die by depositing layers of materials in a precise series of mask steps. The result is a set of six precisely constructed optical channels that offer Gaussian filter characteristics with a full width at half maximum (FWHM) bandwidth of 20 nanometer (nm) for the NIR spectrum AS7263. These filters are precise, smaller, low cost and more stable than using conventional methods.

Interference filter materials and fabrication method makes the device stable over time or temperature.

## 4.6.3 Spectral data collection

The sensor can communicate using both an I<sup>2</sup>C interface and serial interface using AT commands. Its USB can be used to interface directly with the computer and display the spectral data from the sensor with a baud rate of 115200. For the purpose of reading spectral data, we keep the mangosteen sample close enough to the light source so it touches mangosteen surface. The sensor was interfaced via USB to our computer and data was displayed through putty serial port command line. To monitor and analyze system's serial data transmissions, some software tool is required. COM Port Reader allows to read data from serial ports. PuTTY is an open source terminal emulator, used to connect to SSH, telnet and similar servers for remote administration. It also enables to connect to a device attached to the serial port on the computer and displaying the serial data from

the port as shown in Figure 4.7.

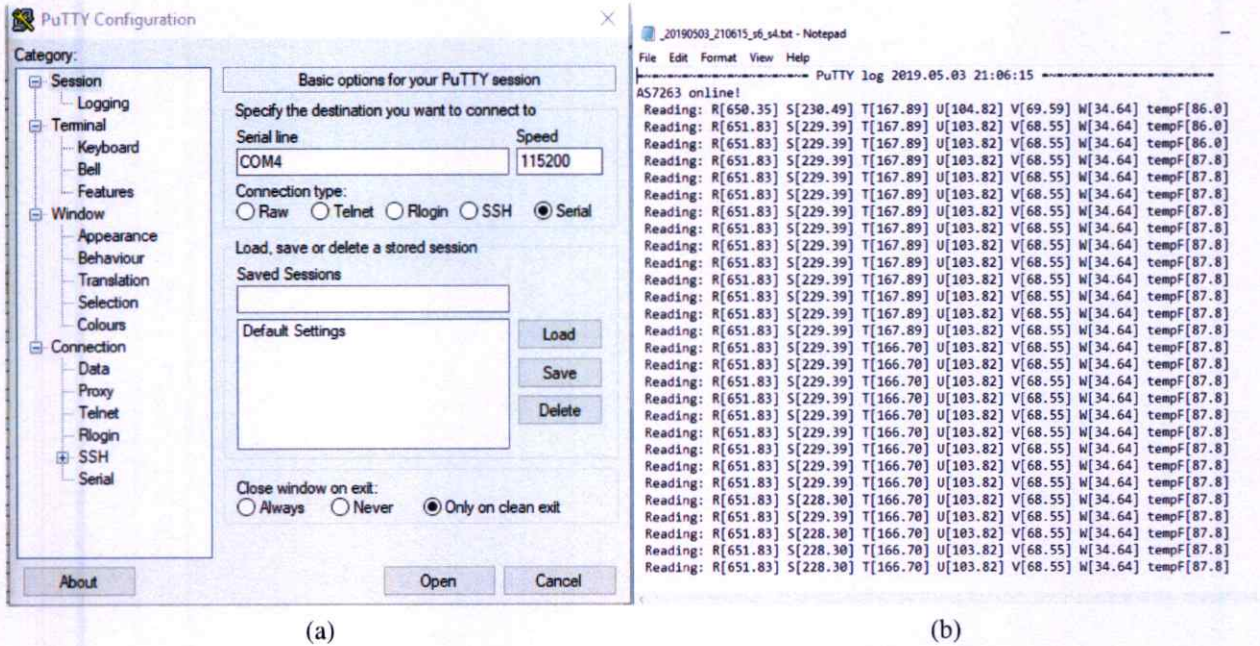


Figure 4.7: Data reading from serial port

## 4.7 Feature Selection

All of the features we find in the dataset might not be useful in building a machine learning model to make the necessary prediction. Using some of the features might even make the predictions worse. So, feature selection plays a huge role in building a machine learning model. We obtain 14 textural features from gray level co occurrence matrix as suggested by [26].

### 4.7.1 Statistical Significance Analysis

Statistical significance is built on a few simple ideas: hypothesis testing, the normal distribution, and  $p$  values. A  $p$ -value is the probability of observing results at least as extreme as those measured when the null hypothesis is true. Once we gathered our results through an experiment, statistical inference allows us to examine evidence in favor or we can claim our idea based on the statistical testing. With aim to study the statistical significance of extracted features we evaluated  $p$ -value of each feature taken from 2 classes. Table 4.4 shows  $p$ -value observation for each

features among three surface classes. From the table, we can come up with the conclusion that features: Correlation ( $f_3$ ), Sum Entropy ( $f_8$ ), Entropy ( $f_9$ ) and Maximal Correlation Coefficient ( $f_{14}$ ) have been found to be significantly different for discriminating each surface class.

Table 4.4: Comparison results of the extracted features.

Extracted Features	<i>p</i> -value		
	GS vs MR	GS vs ER	MR vs ER
Energy	<0.0001	0.0002	<0.0001
Contrast	<0.0001	<0.0001	0.0006
Correlation*	<0.0001	<0.0001	<0.0001
Variance	0.0018	<0.0001	0.6597
Homogeneity	<0.0001	<0.0001	0.0005
Sum Average	0.0002	0.0001	0.5189
Sum Variance	0.0017	<0.0001	0.6588
Sum Entropy*	<0.0001	<0.0001	<0.0001
Entropy*	<0.0001	<0.0001	<0.0001
Difference Variance	<0.0001	<0.0001	0.0006
Difference Entropy	<0.0001	<0.0001	0.0013
Information measure of Correlation I	0.0279	<0.0001	<0.0001
Information measure of Correlation II	<0.0001	0.657	<0.0001
Maximal Correlation Coefficient*	<0.0001	<0.0001	<0.0001

\*Note: significant features highlighted.

Correlation is another statistical term which in commonly refers to how close two variables are to having a linear relationship with each other. Features with high correlation are more linearly dependent and hence have almost the same effect on the dependent variable. So, when two features have high correlation, we can drop one of the two features.

## 4.7.2 Principal Component Analysis

In our study we select important variables. Selecting important variables and removing redundant variables is always helpful and important for the performance of machine learning algorithm. For this purpose we use Principal Component Analysis (PCA) which is based on correlation among attributes. PCA is used to summarize the information in a data set described by multiple variables. The information in a data refers to the total variation it contains. PCA reduces the dimensionality of data containing a large set of variables. This is achieved by transforming the initial variables into a new small set of variables without losing the most important information in the original data set. These new variables corresponds to a linear combination of the originals and are called principal

components.

## **4.8 Classification Tasks**

In this study, there are three approaches used for overall quality grading of mangosteen. It covers surface roughness as external defect and translucent content and yellow gummy latex defect as internal defect.

### **4.8.1 Surface Roughness Classification**

We collected mangosteen samples with 3 levels of surface roughness and then obtain images for each sample and created our image database. Surface roughness is one of the defect in the export industry and its classification is very important. For each sample we extract texture features based on gray level co occurrence matrix and also use deep learning self learned features for classification. Three types surface roughness are encoded using one hot encoding before being trained in convolutional neural network.

### **4.8.2 Internal defects classification**

Internal defects classification is a process of classifying mangosteen as normal sample or as sample with internal defects caused by excessive amount of water in the fruit pulp or presence of yellow gum like substance in the fruit's flesh.

### **4.8.3 Machine Learning Approach**

For the recognition and classification of internal and external defects of mangosteen we want to develop classification model. Machine learning algorithms can perform better if we have data sets with features that are highly distinctive among classes.

## 4.8.4 Random Forest

Random forests (or decision tree forests) are an example of an ensemble learner built on decision trees. Random forests combine versatility and power into a single machine learning approach. As the ensemble uses only a small, random portion of the full feature set, random forests can handle extremely large datasets. Random forest applies the technique of bagging (bootstrap aggregating) to decision tree learners [33].

Random forest is a good option for regression and best known for its performance in classification problems. Some of the advantages of ensemble learning approach of Random Forest are:

- Ensemble learning prevents overfitting of data
- Bootstrapping enables random forest to work well on relatively small datasets and
- Predictors can be trained in parallel
- Decision tree learning enables automatic feature selection

## 4.8.5 Support Vector Machine

Support Vector Machine (SVM) is responsible for finding the decision boundary to separate different classes and maximize the margin. Learning of SVM combines aspects of both the instance-based nearest neighbor learning and the concepts of linear regression, this combination makes SVM powerful, allowing SVMs to model highly complex relationships [33]. SVMs use a boundary called a hyperplane to partition data into groups of similar class values as seen in Figure 4.8. Real data might not be always linearly separable, so SVM address non-linearly separable cases by introducing concepts like Soft Margin and Kernel Tricks. Soft Margin is like finding line to separate, but tolerate one or few misclassification. Whereas Kernel Trick is finding non-linear decision boundary. Kernel trick makes use of existing features and apply some transformations to create new features. Those new features are the key for SVM to find the nonlinear decision boundary. Use of kernels and soft margin powers Support Vector Machine to structure the decision boundary for linear non-separable cases and also effective for multiclass problems.

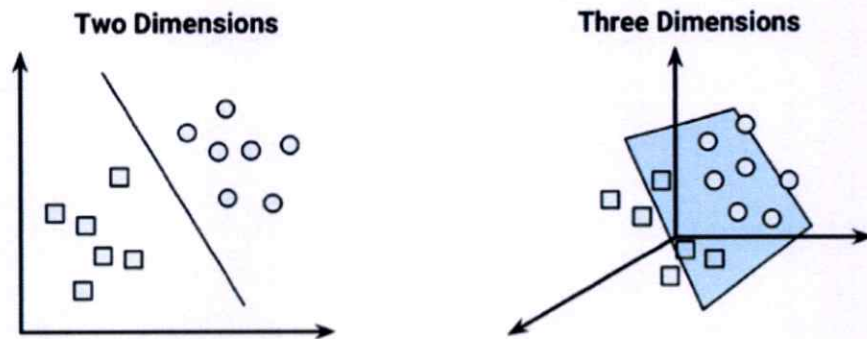


Figure 4.8: Hyperplanes for linearly separable data [33]

### 4.8.6 Performance Evaluation

The goal of evaluating a classification model is to have a better understanding of its performance and to observe how well our proposed method works. In our study performance of SVM and Random Forest classifier has been compared before feature selection and after using selected features based on PCA for surface roughness classification. For internal defect classification based on reflection spectral data we used 3 variants of Support Vector Machine (SVM) namely: Linear, Polynomial and Radial, which is similar to tuning of parameters by changing SVM kernel.

Confusion matrix is a popular way of evaluating performance of classification algorithm. It is a table that categorizes predictions according to whether they match the actual value. Confusion matrix can be created for models that predict any number of class values [33]. In the confusion matrix, each column represents the predicted class whereas each row represents the actual class respectively [34]. Performance measures used for the model evaluation were accuracy and F-measure in our study.

## 4.9 Development Environment

Experiments in this work are partly conducted in MATLAB R2017a and Rstudio.

Confusion Matrix		Predicted		
		Class 1	Class 2	Class 3
Actual	Class 1	A	B	C
	Class 2	D	E	F
	Class 3	G	H	I

True positives
  True Negatives
  Misclassified cases.

Figure 4.9: Confusion Matrix for two-class three-class classification model.

[34]

# Chapter 5

## Experiments and Results

In this section, there will be detailed explanations of the experiments performed in this research. Lastly, the results achieved in the experiment are summarized and discussed.

### 5.1 Experiment 1: Surface Roughness Classification using Texture features

#### 5.1.1 Objective

This experiment measures and compares accuracies of different classifiers used for surface roughness classification of mangosteen with extracted textural features. Performance of SVM and Random forest classifier is compared before and after feature selection by PCA.

#### 5.1.2 Experiment Setup

The experiment is set up as follows:

**Dataset:** This experiment is conducted with the database of images that we created after collection of mangosteen sample. From this image dataset we extracted 14 texture features. We consider all 14 features and use those features for classification. We also performed classification after feature selection based on PCA. Correlation matrix was computed to obtain eigen values and eigen vectors while implementing PCA. There are 802 instances of data. Each instance consists of 14

attributes before feature selection and 3 labelled classes. Description of 3 classes is mentioned in Table 4.1. The data type of all features is integer. For training and testing purpose dataset is randomly divided into 80:20 ratio.

Table 5.1: Details of surface roughness classification dataset

No.	Class	No. of instances	Texture Features
1	GS	252	14
2	MR	232	14
3	ER	318	14

Correlation matrix heatmap of the textural features can be seen in Figure 5.1. In the figure f1-f14 represents 14 textural features extracted from GLCM. There seems to be some features that are highly correlated and such redundant features can be reduced with the application of Principal Component Analysis. Eigenvalues and Eigenvectors were calculated from the correlation matrix. From Table 5.2 we can see that first four Principal Component (PC) have eigenvalues greater than 1 and they contribute to 91% of variance of data. We can see that from 14 features we reduced to four principal components with not much loss of variance. Four principal components were used for the experiment purpose.

Table 5.2: Details of Principal components

No.	Eigenvalue	Proportion	Cumulative
1	2.4054	0.4133	0.4133
2	1.7455	0.2176	0.6309
3	1.5357	0.1685	0.7994
4	1.2608	0.1135	0.9129
5	0.6828	0.0333	0.9462
6	0.6101	0.02659	0.97281
...	...	...	...
14	0.001539	0.0000	1

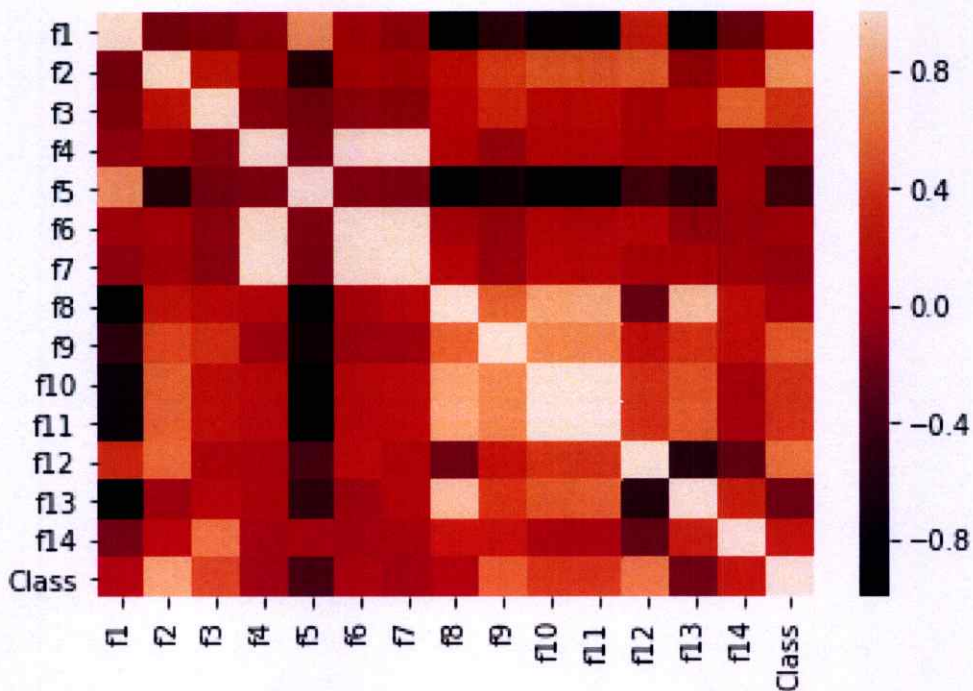


Figure 5.1: Correlation heatmap of texture feature dataset

### 5.1.3 Evaluation Models

The performance of Random Forest and SVM classifier is measured in terms of accuracy and F-measure before and after application of PCA feature selection to classify 3 classes mangosteen surface roughness.

### 5.1.4 Results

Table 5.3 shows the experimental results. We can see the positive effect of feature reduction due to PCA approach on both of the classifier. Both the classifier have improved in terms of accuracy after feature implementing PCA. Number of trees were 500 for Random forest and 3 variables were used for each split. SVM with Radial Basis Function (RBF) kernel was used. With the 'tune' function we optimized hyperparameters like gamma and cost for SVM.

Table 5.3: The comparison of accuracy between SVM and RF with and without PCA

Classifier	14 texture features		Feature selection with PCA	
	Accuracy (%)	F-measure	Accuracy (%)	F-measure
Random Forest	88.23	0.92	92.81	0.92
SVM	90.19	0.90	95.42	0.95

## 5.2 Experiment 2: Surface Roughness Classification using Deep learning

### 5.2.1 Objective

Our motive behind using deep learning is also to compare performance of hand crafted features and self learned features for surface roughness classification. This experiment measures and compares accuracies of simple CNN model trained from scratch with pre-trained CNN model, Resnet50 with different optimizers.

### 5.2.2 Experiment Setup

The experiment is set up as follows:

**Dataset:** This experiment is conducted with the database of images that we created after collection of mangosteen sample. We obtain region of interest by manual cropping of image and resizing it as per the requirement. There are 802 images in our dataset same as mentioned in Table 5.1 with different number of images in each class of surface roughness (GS:252, MR:232, ER:318).

### 5.2.3 Evaluation Models

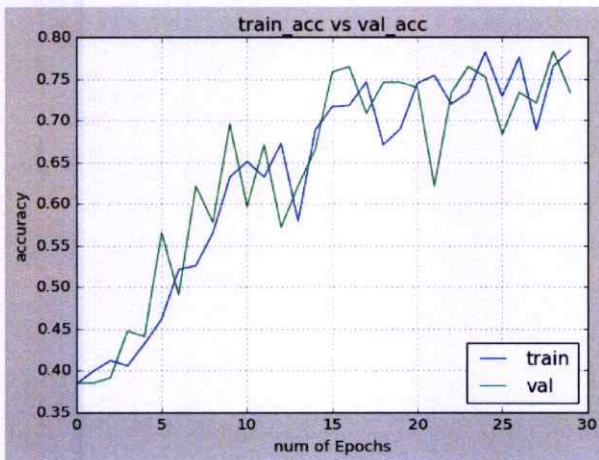
We want to compare between the performance of simple CNN and some pre-trained CNN model. Table 4.2 shows details of CNN model that we build and train from scratch.

## 5.3 Results

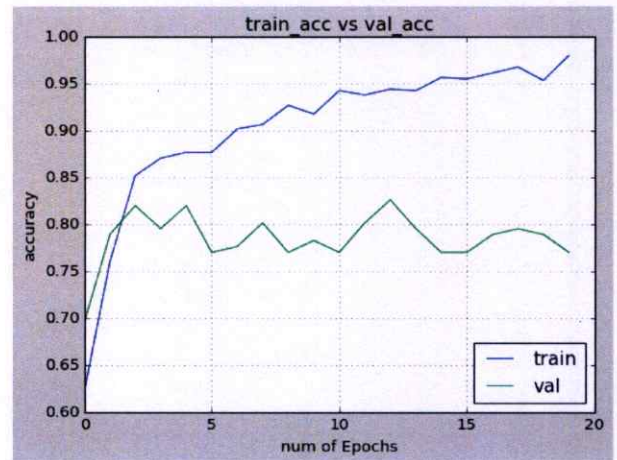
The performance of 2 classifiers is measured in terms of how accurately they classify 3 classes mangosteen surface roughness. Table 5.4 shows the experimental results. From the results depicted in the table we can see that simple CNN which we trained from scratch using our own dataset gives poor performance compared to Resnet50 with both adam and adamax optimizer. Graphical representation of Table 5.4 are shown in Figure

Table 5.4: The Comparison of accuracy between Simple CNN and Resnet50.

Model	Optimizer	F-measure	Testing Accuracy (%)
Simple CNN	Adam	0.73	73.29
Resnet50	Adam	0.77	84.44
Simple CNN	Adamax	0.73	73.29
Resnet50	Adamax	0.83	83.22

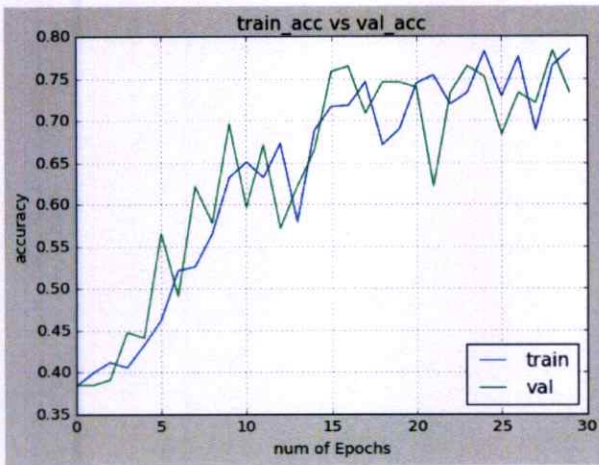


(a)

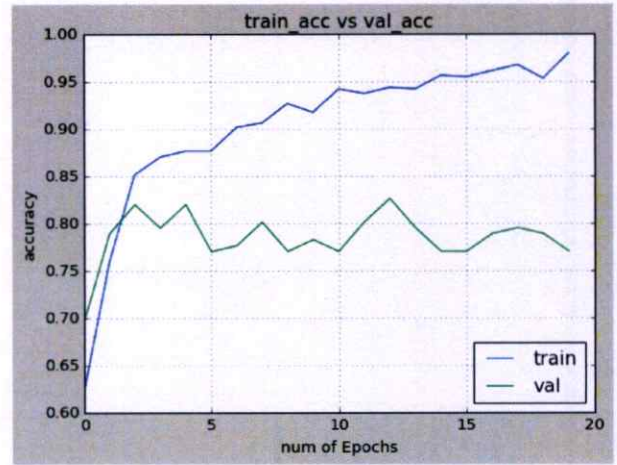


(b)

Figure 5.2: (5.2a) Training Vs Validation accuracy of Simple CNN with Adam optimizer, (5.2b) Training Vs Validation accuracy of Resnet50 with Adam optimizer.



(a)



(b)

Figure 5.3: (5.3a) Training Vs Validation accuracy of Simple CNN with Adamax optimizer, (5.3b) Training Vs Validation accuracy of Resnet50 with Adamax optimizer.

## 5.4 Experiment 3: Internal Defect Classification using NIRS Spectrum

### 5.4.1 Objective

This experiment is conducted to analyse the reflection spectrum of 3 classes in NIR region. If we are able to see the pattern of reflectance at certain wavelength we can have information about difference in composition of 3 classes.

### 5.4.2 Experiment Setup

The experiment is set up as follows:

**Dataset:** This experiment is conducted with the mangosteen samples collected from the farm that was carried to the laboratory. This collection of mangosteen were initially labelled as normal sample, translucent sample and and sample with yellow gummy latex. More information about these classes is explained in Table 4.3. AS7263 is a digital 6-channel spectrometer for spectral identification in the near infrared (NIR) light wavelengths. NIR spectra acquisition was obtained using the spectrometer in NIR region in the range at 610, 680, 730, 760, 810 and 860 nm of light. There are 180 instances of datasets. So for each sample we have 6 attributes which refers to reflection

Table 5.5: Attributes indicated by 6 channels in NIR wavelength and three classes for internal defect classification.

NIR-Channel	Labeled Classes
R (610)	NS (Normal sample)
S (680)	YG (Yellow Gummy latex)
T (730)	TD (Translucent)
U (760)	
V (810)	
W (860)	

wavelength in each channel as shown in Table 5.5

**Nirs spectral acquisition:** We have 3 class of mangosteen sample which is normal (NS), translucent(TD) and yellow gummy latex (YG) defect. In each group there are 15 samples. NIRS data acquisition set up can be depicted in the figure below. Each sample were placed close enough to the light source so as to touch the fruit surface. For each sample we took 4 reading facing each side of calyx. We numbered each calyx and took reading as depicted in Figure 5.4. The reason behind this is to identify which side or part of mangosteen has translucent flesh or gummy latex . After taking reading we wanted to cut open mangosteen to confirm NIR absorption or reflectance pattern for each side and check if defect was there or not. Normal sample and sample with translucent and gummy latex defect will have different concentration of water in the flesh and pericarp. Absorption and reflection of light passed through the sample is different based on the water content and other substance in the flesh and pericarp.

### 5.4.3 Reflection Spectral Analysis

As we have discussed earlier, spectrum analysis relies on identifying the wavelengths reflected by a target which is mangosteen sample in our case. We obtain wavelength of reflected light in each channel as shown in the Figure 4.7b. After taking average of readings obtained in each channel for each class, We evaluate reflectance in each channel and plot against NIR wavelength as depicted in Figure 5.5. Reflectance is defined as the ratio of reflected light to incident light [35]. From this plot we can see that reflectance is higher for TD class compared to YG and NS class in almost all



(a)



(b)

Figure 5.4: NIRS data reading (5.4a) Four sides of a sample numbered through calyx, (5.4b) Sample placed close to light source for NIRS data collection.

channels. Translucent sample has relatively higher water content giving it glass like appearance which gives the name translucent. Due to high water content transmission of light is more than the normal sample. We know from previous studies that SW-NIR transmittance mode shows decreasing absorption around 715nm and fall even down to give negative absorption at 815nm. In Figure 5.5 we can observe that reflectance for TD class is gradually decreasing from S(730) to W(860) channel which might be the effect of higher transmission in this particular wavelength. As we do not have transmission spectral data we can not claim that decreasing reflectance is due to transmission of more light. However without further data and information, we can only conclude to an understanding that reflectance spectral differences between 3 classes of mangosteen in each of the 6 channel were attributed to components changes rather than directly quantifying water content.

#### 5.4.4 Evaluation Model

Details of evaluation models are described in Table 5.6. We use support vector machine (SVM) as classifier to perform the classification of internal defects of mangosteen after taking data for near infrared reflectance wavelength. We compare the performance of SVM with different kernels such as linear, polynomial and radial.

#### 5.4.5 Results

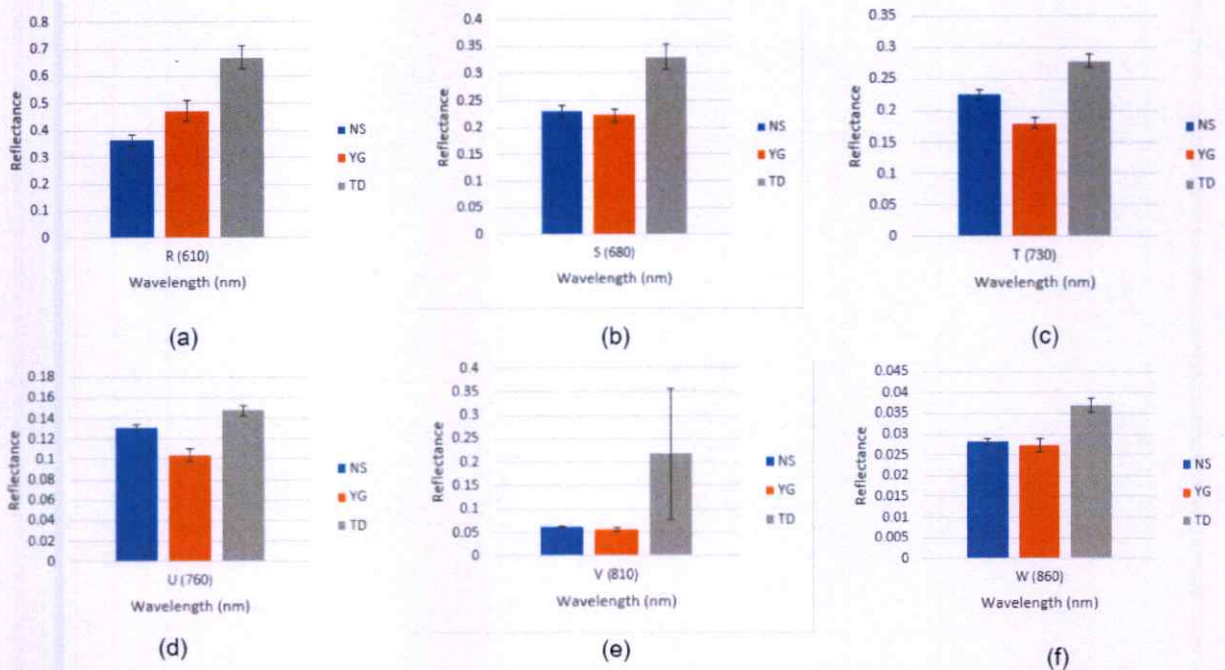


Figure 5.5: Reflectance spectra of 3 classes of mangosteen sample in 6-channels of NIR wavelength at 610, 680, 730, 780, 810 and 860 nanometer (nm) respectively.

Table 5.6: The Comparison of accuracy between variants of SVM

Model	Kernel	K- Fold CV	Classification Accuracy (%)
SVM1	linear	10	80.55
SVM2	polynomial	10	77.77
SVM3	radial	10	83.33
SVM4	sigmoid	10	85.22

Using these reflectance value in each channel as features we build SVM classifier. Performance is measured in terms of accuracy. Classification result of SVM model with different kernel is shown in Table 5.6.

After taking NIR data reading for each class we cut and open mangosteen sample to check internal defects.

# Chapter 6

## Discussion

Our study mainly focuses on non-destructive grading of mangosteen using computer vision, deep learning and NIRS techniques. To perform the fruit grading we take into consideration some common internal and external defects in mangosteen. For the classification of fruit external surface defects, we experiment with texture features obtained from gray level co-occurrence matrix algorithm and self learned features from CNN. Translucent content and presence of yellow gum like substance in the fruit pulp are major internal defects and we focused on using near infrared reflectance spectroscopy (NIRS) for the recognition and classification purpose.

For the grading of mangosteen sample, we performed three experiments. First experiment was based on classifying surface roughness with texture features. We used SVM and Random Forest classifier for the task. First all 14 texture features were used for the classification giving accuracy of 88.23% and 90.19% for SVM and Random forest respectively. As some of the features were related with high correlation, we applied feature reduction technique using Principal Component Analysis. Four principal components were used for the experiment purpose which gave cumulative variance of 91%. Feature reduction showed improvement in performance of both the classifier. In the Second experiment we focused on the use of deep learning and self learned features for the surface roughness classification. We created simple CNN model and trained in from scratch using our dataset. Our main objective was to compare between hand crafted features and self learned features. Classification accuracy of this CNN model was not very promising as compared to SVM or Random Forest classifier which might have caused due to smaller image dataset. Whereas using pretrained CNN model Resnet50 we observed better classification result for surface roughness than

compared to Simple CNN.

The third and final experiment was for determination and classification of internal defects of mangosteen. This experiment is conducted in order to determine the internal defects present in mangosteen. In our study as mentioned earlier we have 3 classes for this purpose as seen in Table 5.5. NS is the class of internal defect free or normal mangosteen. YG is the class with sample having yellow gummy defect and TD is the class with sample having translucent flesh. As these defects are caused by excess of water content and many other chemical components reflectance for each class is different. We can see that class TD has higher reflectance than class YG and class N has lowest reflectance among all. This higher reflectance of NIR light for class TD is seen for almost all channels. We can observe the different pattern of NIR reflectance for 3 classes and group them accordingly. These reflectance pattern are highly discriminative for 3 classes. From results we can see that sigmoid kernel SVM outperforms other svm model with the classification accuracy of 85.22%.

One of the contribution of this study is recognition and classification of surface roughness of mangosteen. This is one of the factor associated with pricing and export of mangosteen. Three classes of surface roughness are suggested by our study based on texture analysis for the first time. Comparison of translucent and yellow gummy latex defect with normal sample based on NIR reflectance spectroscopy is also a novel contribution of our study.

# Chapter 7

## Conclusion

Application of computer vision, deep learning and near infrared spectroscopy has proved to be efficient for overall grading of mangosteen fruit. We compared the performance of SVM and Random forest for surface roughness classification. With all 14 GLCM textural SVM outperforms Random forest with accuracy of 90.19%. After feature reduction with PCA both the classifier performance improves as we can see in Table 5.3 . When compared the performance of Simple CNN model and pretrained Resnet50 model, the latter outperformed the former. NIRS approach was able to give insight about reflectance property of samples of 3 internal defect classes. AS7263-NIR spectrometer identifies spectra in the NIR light wavelengths in the range 610 to 860, which includes the SW-NIR region. As this region has been studied for internal defects in fruits and vegetables we chose the AS7263-NIR spectrometer. For any given mangosteen sample our approach can classify it based on surface roughness into 3 classes GS, MR, and ER respectively. Similarly it can classify based on internal defects into 3 classes NS, TD and YG respectively.

### 7.0.1 Limitations and Future Work

Now we are manually cropping ROI which can be automated using detection algorithm. Absorbance and reflectance of NIR wavelength gives information about different chemical contents inside fruit and each substance respond in different way with NIR spectroscopy. Here we cannot claim that it is only because of higher water content that translucent sample has lower absorbance, it needs to be validated. For now we have considered few defects related to mangosteen. In future

other defects related to mangosteen could be taken into account which could aid the export industry.

*IEEE International Conference on Control System, Computing and Engineering (ICCSCE)*, pp. 242–246, 2017.

- [8] A. Kamalakannan and G. Rajamanickam, “Surface defect detection and classification in mandarin fruits using fuzzy image thresholding, binary wavelet transform and linear classifier model,” in *2012 Fourth International Conference on Advanced Computing (ICoAC)*, pp. 1–6, 2012.
- [9] S. A. Khoje, S. Bodhe, and A. Adsul, “Automated skin defect identification system for fruit grading based on discrete curvelet transform,” *International Journal of Engineering and Technology*, vol. 5, no. 4, pp. 3251–3256, 2013.
- [10] G. Capizzi, G. L. Sciuto, C. Napoli, E. Tramontana, and M. Woźniak, “Automatic classification of fruit defects based on co-occurrence matrix and neural networks,” in *2015 Federated Conference on Computer Science and Information Systems (FedCSIS)*. IEEE, 2015, pp. 861–867.
- [11] K. Vijayarekha and R. Govindaraj, “Citrus fruit external defect classification using wavelet packet transform features and ann,” in *IEEE International Conference on Industrial Technology*, pp. 2872–2877, 2006.
- [12] S. Riyadi, L. M. Azizah, C. Damarjati, T. K. Hariadi *et al.*, “Evaluation of mangosteen surface quality using discrete curvelet transform,” in *2018 International Conference on Information and Communication Technology Convergence (ICTC)*. IEEE, 2018, pp. 475–479.
- [13] T. Pankasemsuk, J. O. Garner, F. B. Matta, and J. L. Silva, “Translucent flesh disorder of mangosteen fruit (*garcinia mangostana* l.),” *HortScience*, vol. 31, no. 1, pp. 112–113, 1996.
- [14] T. Tongleam, N. Jittiwarakul, P. Kumhom, and K. Chamnongthai, “Non-destructive grading of mangosteen by using microwave moisture sensing,” in *IEEE International Symposium on Communications and Information Technology, ISCIT*, vol. 2, pp. 650–653, 2004.
- [15] R. Jaritngam, C. Limsakul, B. Wongkittiserksa *et al.*, “The translucent and yellow gummy latex of mangosteen by using the vfss measurement,” *Journal of Biology, Agriculture and Healthcare*, vol. 2, no. 1, pp. 83–91, 2012.

- [16] T. Yantarasri, J. Sornsrivichai, and P. Chen, "X-ray and nmr for nondestructive internal quality evaluation of durian and mangosteen fruits," in *International Postharvest Science Conference Postharvest 96 464*, 1996, pp. 97–102.
- [17] M. Syah, E. Mansyah, T. Purnama, and D. Fatria, "The control of yellow latex in mangosteen fruit through irrigation and fertilizer application," in *IV International Symposium on Tropical and Subtropical Fruits 975*, 2008, pp. 449–454.
- [18] A. A. F. Joe and A. Gopal, "Identification of spectral regions of the key components in the near infrared spectrum of wheat grain," in *2017 International Conference on Circuit, Power and Computing Technologies (ICCPCT)*. IEEE, 2017, pp. 1–5.
- [19] K. B. Walsh, M. Golic, and C. V. Greensill, "Sorting of fruit using near infrared spectroscopy: application to a range of fruit and vegetables for soluble solids and dry matter content," *Journal of Near Infrared Spectroscopy*, vol. 12, no. 3, pp. 141–148, 2004.
- [20] H. Huang, H. Yu, H. Xu, and Y. Ying, "Near infrared spectroscopy for on/in-line monitoring of quality in foods and beverages: A review," *Journal of food engineering*, vol. 87, no. 3, pp. 303–313, 2008.
- [21] K. Miyamoto and Y. Kitano, "Non-destructive determination of sugar content in satsuma mandarin fruit by near infrared transmittance spectroscopy," *Journal of Near Infrared Spectroscopy*, vol. 3, no. 4, pp. 227–237, 1995.
- [22] C. Clark, V. McGlone, C. Requejo, A. White, and A. Woolf, "Dry matter determination in 'hass' avocado by nir spectroscopy," *Postharvest Biology and Technology*, vol. 29, no. 3, pp. 301–308, 2003.
- [23] G. Birth, "Nondestructive detection of watercore in delicious apples," in *Proc. Am. Soc. Hort. Sci.*, vol. 85, 1964, pp. 74–78.
- [24] A. Terdwongworakul, N. Nakawajana, S. Teerachaichayut, and A. Janhira, "Determination of translucent content in mangosteen by means of near infrared transmittance," *Journal of food engineering*, vol. 109, no. 1, pp. 114–119, 2012.

- [25] E. Ayman, S. M. Hassan, and H.-E. H. Osman, "Mangosteen (*garcinia mangostana* l.)," in *Nonvitamin and Nonmineral Nutritional Supplements*. Elsevier, 2019, pp. 313–319.
- [26] R. M. Haralick, K. Shanmugam *et al.*, "Textural features for image classification," *IEEE Transactions on systems, man, and cybernetics*, no. 6, pp. 610–621, 1973.
- [27] S. Saha. (2018) A comprehensive guide to convolutional neural networks. [Online]. Available: <https://towardsdatascience.com/a-comprehensive-guide-to-convolutional-neural-networks-the-eli5-way-3bd2b1164a53>
- [28] A. Davies, "An introduction to near infrared (nir) spectroscopy," *A Journal of Near Infrared Spectroscopy*, vol. 16, pp. 9–11, 2014.
- [29] R. Mills. (2017) Nir technology for routine analysis of food and agricultural products. [Online]. Available: <https://www.fossanalytics.com/en/news-articles/technologies/nir-technology>.
- [30] AMS. As7263 6-channel nir spectral id device with electronic shutter and smart interface. [Online]. Available: <https://www.mouser.co.uk/new/ams/ams-as7263-spectral-id-device/>
- [31] J. Y. Tou, P. Y. Lau, and Y. H. Tay, "Computer vision-based wood recognition system," 2007.
- [32] A. A. Almisreb, N. Jamil, and N. M. Din, "Utilizing alexnet deep transfer learning for ear recognition," in *Fourth International Conference on Information Retrieval and Knowledge Management (CAMP)*. IEEE, 2018, pp. 1–5.
- [33] B. Lantz, *Machine learning with R*. Packt Publishing Ltd, 2009.
- [34] M. Ali, D.-H. Son, S.-H. Kang, and S.-R. Nam, "An accurate ct saturation classification using a deep learning approach based on unsupervised feature extraction and supervised fine-tuning strategy," *Energies*, vol. 10, no. 11, p. 1830, 2017.
- [35] T. A. Germer, J. C. Zwinkels, and B. K. Tsai, "Theoretical concepts in spectrophotometric measurements," in *Experimental Methods in the Physical Sciences*. Elsevier, 2014, vol. 46, pp. 11–66.



## Highlight theme : Automated Machine Learning, Deep learning & Generative models for Smarter Living

21-24 November 2018, Chiang Mai, Thailand

### Call For Paper

The International Computer Science and Engineering Conference (ICSEC) is the premier forum for the presentation of technological advances and research results in the fields of Computer Science, Computer Engineering, Information Technology, and Emerging Intelligent Technology. ICSEC 2018, will be held over three days, with tutorial sessions and presentations delivered by researchers from the international communities, including presentations from well-known keynote speakers. In this special year, ICSEC2018 will be held in conjunction with the 11th Biomedical Engineering International Conference (BMEiCON 2018). For international track, conference content will be submitted for inclusion into IEEE Xplore as well as other Abstracting and Indexing (A&I) databases. In addition, the authors of the selected papers in international track will be invited to extend their works for the submission to many journals which are indexed by SCOPUS, ISI, EI, etc.

#### Topic include, but not limit to:

Ad-Hoc Networks	Distributed Computing and Grid Computing	Network Protocol and Architecture
Algorithmic Information	Embedded Systems	Pattern Recognition
Theory Analysis of Algorithms and Problem Complexity	Evolutionary Computing	Pervasive and Mobile Computing
Artificial Intelligence	Formal Semantics	Programming Language
Augmented Reality	Future Internet	Quality of Service, Scalability and Performance
Bioinformatics	Fuzzy and Neural Network Systems	Robotics and Automation
Cloud Computing	Genetic Algorithms	Security and Access Control
Computability Theory	High Performance Computing	Self-Organizing Networks and Networked Systems
Computer and Internet Application	Human Machine Interface	Semantic Web, Ontology
Computer Architecture	Information Technology Management	Simulation and Modeling
Computer Graphics	Intelligent Systems	Social Network Applications
Computer Networks	Internet Modeling	Speech Recognition
Computer Vision and Image Processing	IT Safety and Healthcare	Swarm Intelligent
Computer System Implementation	Knowledge Discovery	Theory of Computation
Control structures and Microprogramming	Knowledge Management	VLSI design
Cryptography and Security	Machine Intelligence and Applications	Web Modeling and Design
Data and Knowledge Management	Mobile Applications	Web Services Architecture
Data Mining	Mobile Computing	Wireless Network and Communication
Decision Support Technologies	Mobile Security	XML-Based Languages
Digital Forensics	Mobile Social Networks	
Digital Signal Processing	Natural Language Processing	
	Network Management	

**Conference Information:** available on <http://icsec2018.org>. Contact us at: [icsec2018.org@gmail.com](mailto:icsec2018.org@gmail.com)

**General Chair:** Ekkarat Boonchieng, CMU, [ekkarat@ieee.org](mailto:ekkarat@ieee.org)

**Local Arrangement Chair:** Varin Chaovatut, CMU

**General Secretary:** Anusorn Chaikaew, CRRU, [anusorn@ieee.org](mailto:anusorn@ieee.org)

#### Important Dates

Submission Deadline	August 31, 2018
Notification of Acceptance	September 15, 2018
Submission of Camera-ready Papers Deadline	October 15, 2018
Early-bird Registration Deadline	October 15, 2018

#### Organized by



Center of Excellence in

**Community Health Informatics**

"Empowering Community by Big Data"



**IEEE**  
THAILAND SECTION

# Surface Roughness Classification of Mangosteen with Gray Level Co-occurrence Matrix based Texture Analysis

Anjali Acharya and Montri Phothisonothai  
*International College*

*King Mongkut's Institute of Technology Ladkrabang*  
Bangkok 10520, Thailand  
E-mail: 60610020@kmitl.ac.th, montri.ph@kmitl.ac.th

Suchada Tantisatirapong

*Department of Biomedical Engineering*  
*Srinakharinwirot University*  
Ongkharak, Nakhon Nayok 26120, Thailand  
E-mail: suchadat@g.swu.ac.th

**Abstract**—Mangosteen is one of the fruits that has an enormous export potential in Thailand. It is well-known as the queen of fruit. Mangosteen export generates large revenue; however, fruit is not defect free it contains many undesirable external as well as internal condition which results in the shipment rejection and decrease the reliability of the export. Therefore, this research investigates an approach for texture image analysis based surface roughness detection and classification into 3 classes: i.e., Glossy Surface, Mid Rough Surface and Extreme Rough Surface. In this study, for the first time, we propose the textural features extracted using Gray-Level Co-occurrence Matrix (GLCM) for surface roughness classification of mangosteen.

**Index Terms**—nondestructive method, mangosteen, texture analysis, image processing, GLCM

## I. INTRODUCTION

The purple mangosteen (*Garcinia mangostana*) is considered one of the well-known tropical fruits grown in South East Asia. For Thailand, this fruit export revenue hits almost 64 million USD in 2011 [1]. However, a problem currently facing by mangosteens gardeners/exporters is that there is still a lack of accurate and practical inspection technology to assure the irregular quality of the mangosteen. The quality of mangosteen fruit is measured by external factors such as color, shape, skin blemishes which are also very important for consumer acceptance [2]. This approach is based on texture analysis of color images to classify surface roughness. Three classes of surface roughness are: glossy, medium rough and rough. Textures are characteristic intensity variations that typically originate from roughness of object surfaces [3]. Generally, it can be defined as a regular repetition of elements or pattern on a surface. These texture images vary in brightness, color, shape, size, etc [3]. Texture analysis is important in many applications of computer image analysis for classification or segmentation of images based on local spatial variations of intensity or color. A feature is an image characteristic that can capture certain visual property of the image. Many results are published, in which image processing is used to assess some particular

quality features based on color, texture and morphology in fruit grading. Image processing techniques have been widely used for surface inspection and grading of fruits. Machine vision systems for visual sizing and color are fairly used in the food processing industry. The surface defects or diseases appearing on the fruits are characterized by different texture patterns [7]. Machine vision system with effective image processing methods are used in quality grading of agricultural products. A pattern recognition techniques was developed to detect and classify surface defects such as pitting, splitting and stem-end rot found in images of mandarin fruits [8]. Suchitra A. Khoje developed an evaluation methodology for quality of fruit surfaces with the classification of Probabilistic Neural Network (PNN) and Support Vector Machine (SVM) [9]. PNN is one of artificial neural network architecture. S. Limsiroratana et.al [10] presented image analysis for harvesting tropical fruits. The method uses matching process to determine all likelihood. It takes a long time, because we have to inverse Fourier series and deform the parameters as many as possible to get enough accurate result. C. Damarjati et.al. used one of deep learning architecture that is Convolutional Neural Network (CNN) for mangosteen surface defect detection. CNN proved to be very efficient regarding classifying images [7]. However, the image processing based classification of mangosteen requires more effective features. The nondestructive method for classification of mangosteen using texture analysis is still technical challenging issue. Research has been done for automatic classification of fruit defects. The texture and gray features of defect area are extracted by computing a gray level cooccurrence matrix and then defect areas are classified by the applied Radial Basis Probabilistic Neural Network (RBPNN) solution [11].

Therefore, we initially aim to propose the texture analysis on the basis of expert-like surface roughness classification using Gray-Level Co-occurrence Matrix (GLCM) method. The proposed method can be described as the following parts:

## II. MATERIAL AND PROPOSED METHOD

In this experiment, we have classified mangosteen sample into 3 classes based on surface roughness from the knowledge

of expert farmers. Postharvest damage in fresh mangosteens at wholesale level in Thailand was investigated from April to October. Total of 37.1% of the production yield was rendered inedible by damage during this period; damages included fruit cracking, hardened rinds, rough surfaces, translucent flesh, gummosis and decay [2]. Three classes can be listed based on heuristic expert knowledge definition in Table I. The system overview of the proposed method is shown in Fig. 1.

TABLE I: Class description

Surface Class	Description
Glossy (GS)	Fine smooth surface with very minimum or no skin bruises. This class gets more consumers preference and pricing is highest.
Medium Rough (MR)	Coarse surface. This class gets lower consumers preference and pricing lower to glossy. Acceptable for export.
Extreme Rough (ER)	Degree of coarseness is higher than medium rough class. Unpleasant to touch, lower consumer acceptance and mainly sold in local markets. Not for export.

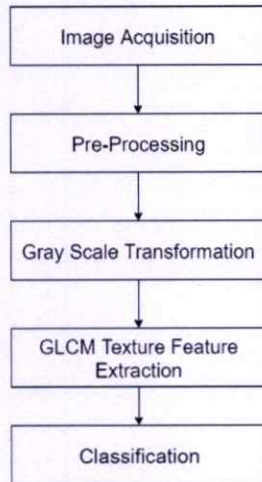


Fig. 1: System overview of the proposed method.

### A. Image Acquisition

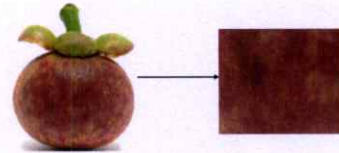
Primary data in this stage is the mangosteen image. Experts/farmers initially sort mangosteen and the same are taken as samples for image acquisition we visited Wangmai sub-district, Chanthaburi province and visited mangosteen farm. We have manually sorted mangosteens surface defected images. All the sample images will be cropped manually and obtain region of interest (ROI). For the manually sorted mangosteen samples image is acquired using Canon G3X digital camera with UDIOBOX III original dimmer lightbox studio. Each image dataset will be taken by high resolution of digital camera: i.e.,  $5,472 \times 3,648$  pixels, as shown in Fig. 2.

### B. Pre-processing

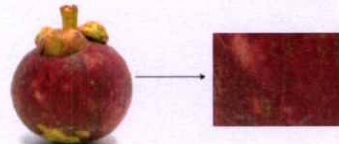
Digital images are prone to various types of noise which might have resulted from our flaws during image acquisition process. Such noise reduces the quality of our image and lead



(a)



(b)



(c)



(d)

Fig. 2: (2a) Image acquisition at mangosteen farm, Wangmai sub-district, Chanthaburi province. Manually cropped ROI to three classes: (2b) Glossy surface (GS class), (2c) Mid-rough surface (MR class), (2d) Extreme rough surface (ER class).

to inaccurate results. After we have our region of interest before we do further processing, we attempt to remove noise from our data using Median filter. Then we resize all images to same dimension which is  $512 \times 512$  pixels.

### C. Gray Level Co-occurrence Matrix (GLCM) Method

Gray level co-occurrence matrix (GLCM) was suggested by Haralick et al. [4]. It is one of the widely used texture analysis algorithm because it can be implemented easily. In statistical texture analysis, textural features are computed from the statistical distribution of observed combinations of intensities at specified positions relative to each other in the image. According to the number of intensity points (pixels) in each combination, statistics are classified into first-order, second-order and higher-order statistics. The GLCM method is a way

of extracting second-order statistical texture features [5]. In this experiment, we applied the color to 8-bit gray conversion formula. The GLCM functions characterize the texture of an image by calculating how often pairs of pixel with specific values and in a specified spatial relationship occur in an image. These features are generated by calculating the features for each one of the co-occurrence matrices obtained by using the directions  $0^\circ$ ,  $45^\circ$ ,  $90^\circ$ , and  $135^\circ$ , and pre-determined distance of relation, then averaging these four values.

#### D. GLCM based Feature Extraction Method

An input color image is transformed into grayscale image. In photography, computing, and colorimetry, a grayscale or grey-scale image is one in which the value of each pixel is a single sample representing only an amount of light, that is, it carries only intensity information. For textural features of mangosteens surface roughness, we will be using GLCM which is a statistical method of examining texture that considers the spatial relationship of pixels [6]. All the 14 GLCM textural features suggested by Haralick et al. has been used in this work. The equations which define a set of 14 measures of textural features are given [4].

##### Notation

$p(i, j)$   $p(i, j)$ th entry in a normalized gray-tone spatial dependence matrix,  $= P(i, j)/R$

$R$  is the normalizing constant.  $R = \sum_{i,j=1}^{N_g} P(i, j)$ .

$p_x(i)$   $i$ th entry in the marginal-probability matrix

$N_g$  Number of distinct gray levels in the quantized image.

Textural Features:

##### 1) Angular Second Moment (Energy)

$$f_1 = \sum_i \sum_j \{p(i, j)\}^2.$$

##### 2) Contrast

$$f_2 = \sum_{n=0}^{N_g-1} n^2 \left\{ \sum_{i=1}^{N_g} \sum_{j=1}^{N_g} p(i, j) \right\}.$$

##### 3) Correlation

$$f_3 = \frac{\sum_{i,j} (ij) p(i, j) - \mu_x \mu_y}{\sigma_x \sigma_y}$$

where  $\mu_x$ ,  $\mu_y$ ,  $\sigma_x$  and  $\sigma_y$  are the means and standard deviations of  $p_x$  and  $p_y$

##### 4) Variance

$$f_4 = \sum_{i,j} (i - \mu)^2 p(i, j).$$

##### 5) Inverse Difference Moment (Homogeneity)

$$f_5 = \sum_i \sum_j \{p(i, j)\}^2.$$

##### 6) Sum Average

$$f_6 = \sum_{i=2}^{2N_g} i p_{x+y}(i).$$

##### 7) Sum Variance

$$f_7 = \sum_{i=2}^{2N_g} (i - f_8)^2 p_{x+y}(i).$$

##### 8) Sum Entropy

$$f_8 = - \sum_{i=2}^{2N_g} p_{x+y}(i) \log \{p_{x+y}(i)\}.$$

##### 9) Entropy

$$f_9 = - \sum_{i,j} p(i, j) \log(p(i, j)).$$

##### 10) Difference Variance

$$f_{10} = \text{Var of } p_{x-y}.$$

##### 11) Difference Entropy

$$f_{11} = - \sum_{i=0}^{N_g-1} p_{x-y}(i) \log \{p_{x-y}(i)\}.$$

##### 12) Information Measure of Correlation I

$$f_{12} = \frac{H(X, Y) - H(X, Y)_1}{\max \{H(X), H(Y)\}}.$$

##### 13) Information Measure of Correlation II

$$f_{13} = (1 - \exp[-2.0(H(X, Y)_2 - H(X, Y))])^{\frac{1}{2}},$$

$$H(X, Y) = - \sum_{i,j} p(i, j) \log(p(i, j)).$$

where  $H(X)$  and  $H(Y)$  are entropies of  $p_x$  and  $p_y$ , and

$$H(X, Y)_1 = - \sum_{i,j} p(i, j) \log \{p_x(i) p_y(j)\},$$

$$H(X, Y)_2 = - \sum_{i,j} p_x(i) p_y(j) \log \{p_x(i) p_y(j)\}.$$

##### 14) Maximal Correlation Coefficient

$$f_{14} = (\text{Second largest eigenvalue of } Q)^{\frac{1}{2}},$$

where

$$Q(i, j) = \sum_k \frac{p(i, k) p(j, k)}{p_x(i) p_y(k)}.$$

### III. EXPERIMENTAL RESULTS AND DISCUSSIONS

In this experiment, we used Matlab and RStudio for offline analysis: 165 samples of Mangosteen surface images, 55 samples for each surface roughness. GLCM function with a horizontal offset of 1 and average value of four directions  $0^\circ$ ,  $45^\circ$ ,  $90^\circ$ , and  $135^\circ$  are computed. We can specify other pixel spatial relationships using the 'Offsets' parameter. The 14 textural features of the GLCM matrices for different classes of surface of Mangosteen are obtained.

For most of the research and study that involved texture analysis based on GLCM, mainly extracted textural features are Contrast, Correlation, Energy and Homogeneity. These four features might not be statistically significant for all

classes, so we choose to extract all suggested textural features and then evaluate their significance. Once we have gathered our results through an experiment, statistical inference allows us to examine evidence in favor or we can claim our idea based on the statistical testing. With aim to study the statistical significance of extracted features we evaluated  $p$ -value of each feature taken from 2 classes. Table II shows  $p$ -value observation for each features among three surface classes. From the table, we can come up with the conclusion that features: Correlation ( $f_3$ ), Sum Entropy ( $f_8$ ), Entropy ( $f_9$ ) and Maximal Correlation Coefficient ( $f_{14}$ ) have been found to be significantly different for discriminating each surface class.

TABLE II: Comparison results of the extracted features.

Extracted Features	$p$ -value		
	GS vs MR	GS vs ER	MR vs ER
Energy	<0.0001	0.0002	<0.0001
Contrast	<0.0001	<0.0001	0.0006
Correlation*	<0.0001	<0.0001	<0.0001
Variance	0.0018	<0.0001	0.6597
Homogeneity	<0.0001	<0.0001	0.0005
Sum Average	0.0002	0.0001	0.5189
Sum Variance	0.0017	<0.0001	0.6588
Sum Entropy*	<0.0001	<0.0001	<0.0001
Entropy*	<0.0001	<0.0001	<0.0001
Difference Variance	<0.0001	<0.0001	0.0006
Difference Entropy	<0.0001	<0.0001	0.0013
Information measure of Correlation I	0.0279	<0.0001	<0.0001
Information measure of Correlation II	<0.0001	0.657	<0.0001
Maximal Correlation Coefficient*	<0.0001	<0.0001	<0.0001

\*Note: significant features highlighted.

#### IV. CONCLUSIONS

In this paper, we have successfully extracted textural features using GLCM. We also found that based on the observed  $p$ -value, four textural features Correlation, Sum Entropy, Entropy and Maximal Correlation Coefficient were statistically significant. For the further study, other feature selection algorithms will be investigated that would help us rank important features. Based on these statistical features of fruit surface, we aim to build a classification model that would help in automatic grading of mangosteen based on surface roughness.

#### V. ACKNOWLEDGMENTS

This research was supported by the International College, King Mongkut's Institute of Technology Ladkrabang, Grant No. 2561-0111003. The authors would like to thank experienced farmer at the mangosteen farm, Wangmai sub-district, Chanthaburi province who helped in this experiment and for grading the class of surface.

#### REFERENCES

- [1] P. Rujapha, C. Kosin, "Nondestructive Exported Mangosteen Grading by Inspection of External Features", *IEEE International Symposium on Communications and Information Technology*, pp 465-468, 2004.
- [2] B. Jarimopas, P. Pushpariksha S. Paul Singh "Postharvest Damage of Mangosteen and Quality Grading Using Mechanical and Optical Properties as Indicators", *International Journal of Food Properties*, Vol.12, pp 414-426, 2009.
- [3] G. Arockia Selva Saroja, C. Helen Sulochana "Texture Analysis of Non-Uniform Images using GLCM", *IEEE Conference on Information Communication Technologies*, pp 1319-1322, 2013.
- [4] R.M. Haralick, K. Shanmugam, I. Dinstein, "Textural Features for Image Classification", *IEEE Transactions on Systems, Man, and Cybernetics*, Vol. 3, No. 6, pp 610621, 1973.
- [5] F. Albreghsen "Statistical Texture Measures Computed from Gray Level Cooccurrence Matrices", Image Processing Laboratory, Department of Informatics, Oslo University Hospital, 1995.
- [6] R. Korchiyne, S. Mohamed Farssi, A. Sbihi, R. Touahni, M. Alaoui, "A Combined Method of Fractal and GLCM Features For MRI And CT Scan Images Classification", *Signal and Image Processing: An International Journal (SIPIJ)*, Vol. 5, No.4, 2014.
- [7] L. Marifatul Azizah, S. Fadillah Umayah, S. Riyadi, C. Damarjati, N. Ananda Utama, "Deep Learning Implementation using Convolutional Neural Network in Mangosteen Surface Defect Detection", *IEEE International Conference on Control System, Computing and Engineering (ICCSCCE)*, pp 242-246, 2017.
- [8] A. Kamalakannan et al "Surface Defect Detection and Classification in Mandarin Fruits using Fuzzy Image Thresholding, Binary Wavelet Transform and Linear Classifier Model". *IEEE Fourth International Conference on Advanced Computing (ICoAC)*, 2012.
- [9] S.A. Khoje, S.K. Bodhe, A. Adsul, "Automated Skin Defect Identification System for Fruit Grading Based on Discrete Curvelet Transform", *International Journal of Engineering and Technology (IJET)*, vol. 5, no. 4, pp. 3251-3256, 2013.
- [10] S. Limsiroratana, Y. Ikeda. "On Image Analysis for Harvesting Tropical Fruits.", *SICE Annual Conference*, Vol. 2, pp 1336-1341, Osaka, Japan, 2002.
- [11] G. Capizzi, G.L. Sciuto, C. Napoli, E. Tramontana and M. Wozniak, "Automatic Classification of Fruit Defects based on Co-Occurrence Matrix and Neural Networks", *Proceedings of the Federated Conference on Computer Science and Information Systems*, Vol. 5, pp. 861-867, 2015.

# Bibliography

- [1] P. Rujapha and C. Kosin, "Nondestructive exported mangosteen grading by inspection of external features," in *IEEE International Symposium on Communications and Information Technology, ISCIT*, vol. 1, pp. 465–468, 2004.
- [2] B. Jarimopas, P. Pushpariksha, and S. P. Singh, "Postharvest damage of mangosteen and quality grading using mechanical and optical properties as indicators," *International Journal of Food Properties*, vol. 12, no. 2, pp. 414–426, 2009.
- [3] N. Nakawajana, A. Terdwongworakul, and S. Teerachaichayut, "Minimally destructive assessment of mangosteen translucency based on electrical impedance measurements," *Journal of Food Engineering*, vol. 171, pp. 137–144, 2016.
- [4] S. Mohana and C. Prabhakar, "Automatic detection of surface defects on citrus fruit based on computer vision techniques," *International Journal of Image, Graphics and Signal Processing*, vol. 7, no. 9, p. 11, 2015.
- [5] S. Hong and D. Huidong, "Fractal dimension applied in texture feature extraction in x-ray chest image retrieval," in *IEEE International Conference on Information and Automation*, pp. 841–845, 2012.
- [6] G. A. S. Saroja and C. H. Sulochana, "Texture analysis of non-uniform images using glcm," in *2013 IEEE Conference on Information & Communication Technologies*, pp. 1319–1322, 2013.
- [7] L. M. Azizah, S. F. Umayah, S. Riyadi, C. Damarjati, and N. A. Utama, "Deep learning implementation using convolutional neural network in mangosteen surface defect detection," in *7th*